Reconstructing the evolutionary history of freshwater fishes (Nemacheilidae) across Eurasia since early Eocene

Vendula Šlechtová[1], Tomáš Dvořák[1,2], Jörg Freyhof[3], Maurice Kottelat[4], Boris Levin[5,6], Alexander Golubtsov[6], Vlastimil Šlechta[1], Jörg Bohlen[1§]

[1]Laboratory of Fish Genetics, Institute of Animal Physiology and Genetics, Academy of Sciences of the Czech Republic, Liběchov, Czech Republic

[2] Department of Zoology, Faculty of Science, Charles University, Prague, Czech Republic

[3] Museum für Naturkunde, Leibniz Institute for Evolution and Biodiversity Science, 10115 Berlin, Germany.

[4] Rue des Rauraques 6, 2800 Delémont, Switzerland (permanent address) and Lee Kong Chian Natural History Museum, National University of Singapore, Singapore

[5] Papanin Institute of Biology of Inland Waters, Russian Academy of Sciences, Borok, Yaroslavl Region, Russia

[6] A.N. Severtsov Institute of Ecology and Evolution of the Russian Academy of Sciences, Moscow, Russia

[§] Corresponding author

Author information:
Vendula Šlechtová: 0000-0002-5499-7550; v.slechtova@iapg.cas.cz
Tomáš Dvořák: 0000-0001-8151-2144; dvorak@iapg.cas.cz
Jörg Freyhof: 0000-0002-7042-3127; joerg.freyhof@mfn.berlin
Maurice Kottelat: 0000-0003-3638-2824; mkottelat@dplanet.ch
Boris Levin: 0000-0002-4044-2036; borislyovin@mail.ru
Alexander Golubtsov: 0000-0002-8317-7527; sgolubtsov@gmail.com
Jörg Bohlen: 0000-0003-1259-008x; joerg_bohlen@yahoo.de

Abstract

Eurasia has undergone substantial tectonic, geological, and climatic changes throughout the Cenozoic era, primarily associated with tectonic plate collisions and a global cooling trend. The evolution of present-day biodiversity unfolded in this dynamic environment, characterised by intricate interactions of abiotic factors. However, comprehensive, large-scale reconstructions illustrating the extent of these influences are lacking. We reconstructed the evolutionary history of the freshwater fish family Nemacheilidae across Eurasia and spanning most of the Cenozoic era. Molecular phylogeny uncovered six major clades within the family, along with numerous unresolved taxonomic issues. Dating of cladogenetic events and ancestral range estimation traced the origin of Nemacheilidae to Indochina around 48 million years ago. Subsequently, one branch of Nemacheilidae colonised eastern, central, and northern Asia, as well as Europe, while another branch expanded into the Burmese region, the Indian subcontinent, the Near East, and northeast Africa. These expansions were facilitated by tectonic connections, favourable climatic conditions, and orogenic processes. Conversely, aridification emerged as the primary cause of extinction events. Our study marks the first comprehensive reconstruction of the evolution of Eurasian freshwater biodiversity on a continental scale and across deep geological time.

Introduction

The present-day species- and genus-level diversity on earth is mainly the result of the evolution during Cenozoic, when biodiversity recovered from the Cretaceous-Tertiary mass extinction event, which eradicated three-quarters of all animal and plant species. During the Cenozoic new lifeforms flourished; often from lineages that had played only a minor role before the mass extinction; like mammals, birds and teleost fishes (Feduccia, 1995; Friedman, 2010).

The Cenozoic is also a period of significant and relatively rapid climatic and geological changes (Summerhayes, 2015). The biggest geological changes occurred in Eurasia, resulting from its collision with the African, Arabian and Indian plates, that caused the closure of the Tethys Sea and the Alpine - Himalayan orogeny (Trifonov et al., 2012). The climate also changed dramatically during Cenozoic; transitioning Earth from a warm and humid greenhouse state to a cool and dry icehouse; but with a complex interplay of large-scale changes and smaller-scale fluctuations, creating a diverse range of climatic conditions on the local scale (Mudelsee et al., 2014).

Geologic and climatic changes are major drivers of biodiversity evolution (Antonelli et al., 2018; Mayhew et al., 2012; Fritz et al., 2016). Numerous biogeographical studies show distribution patterns and local vicariance and radiation events in the Eurasian biodiversity (e.g. Andreyenkova et al., 2021; Ishii et al., 2023). The majority of these studies focused on terrestrial fauna and flora, but we believe that the best suited model organisms for biogeographical analysis are strict

freshwater species. Such hololimnic species are confined to a certain water body unless a physical connection with another water body appears. At the same time, the evolution of the earth's hydrographic network bases on local geological and climatic conditions. The locally 'locked' freshwater fauna thus reflects the environmental past of any region on earth in much more detail than most terrestrial animals or plants (e.g. Bănărescu, 1992; Bohlen et al., 2020a).

Despite this potential, there is a paucity of research on the evolutionary history of Eurasian freshwater biodiversity covering the large geographic and temporal scales. Numerous studies deal with certain geologic or climatic changes during short parts of the Cenozoic (e.g. Kahlke 2014; Ballarin & Li 2018; Gu et al. 2022) or cover a comparably small region of Eurasia (e.g. Delić et al. 2020; Deng et al. 2020; Saito et al. 2018), but there is no comprehensive, overarching analysis that covers the whole of Eurasia, most of the Cenozoic and considers climatic as well as geologic events as driving forces for the evolution of biodiversity.

For the present study we chose the species-rich (> 700 species) freshwater fish family Nemacheilidae (stone loaches) as model; which is omnipresent in almost all water bodies of Europe and Asia (Kottelat, 2012; Dvořák et al., 2022a) and stretches from Spain to Japan in west-east direction and from Russia to indonesia in north-south direction. Most species are small (< 12 cm SL), benthic and inhabit streams and rivers, although some are found in swamps, caves and lakes. Few even occupy extreme environments: Nemacheilidae include the deepest freshwater cave fish in the world (*Triplophysa gejiuensis*, 400 m below surface) and the fish living at

the highest altitude (*Triplophysa stolickai*, 5200 m a.s.l.) (Chu & Chen 1979, Kottelat 2012).

The aim of the study is to reconstruct the evolutionary history of the family Nemacheilidae as example for the evolution of freshwater fauna across Eurasia and since early Cenozoic. The research concept includes a phylogenetic reconstruction based on molecular genetic data, followed by the dating of cladogenetic events and a biogeographic analysis in order to reconstruct ancestral distribution ranges. The results are compared with the known geological and climatic history of Eurasia to identify the causative factors and processes that have influenced the diversification of Eurasian freshwater fishes.

Results

Major clades within Nemacheilidae

To understand the phylogenetic diversity of the family Nemacheilidae and to identify the largest units within, we analysed sequence data for one mitochondrial (cytochrome b) and up to five nuclear (EGR3, IRBP2, Myosin6, RAG1, Rhodopsin1) genes of 471 specimens representing 279 species and 37 genera from across Eurasia (Fig. 1; Supplementary Material Table S1). This is by far the most comprehensive genetic dataset of Nemacheilidae ever published. The outgroup included 21 species from 9 related families (Fig. 2). We applied maximum likelihood analysis (ML) in IQ-TREE and Bayesian inference (BI) in mrBayes on the

concatenated dataset. Besides, the individual unrooted ML gene trees were reconstructed in IQ-TREE and subsequently used as input files for ASTRAL III (Zhang et al., 2018) to infer species tree. All analyses revealed Nemacheilidae as monophyletic group and recovered the presence of six monophyletic major clades within the dataset.

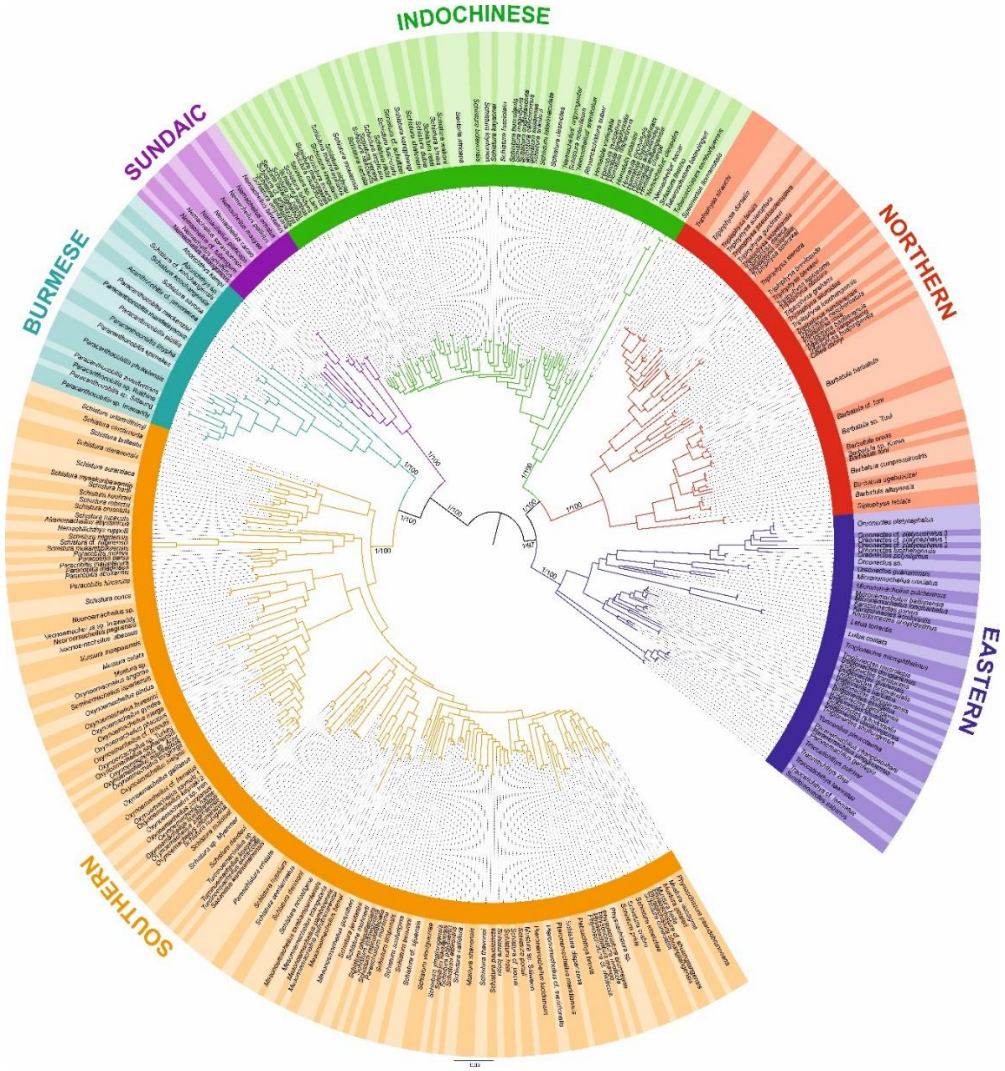

Fig. 1. Phylogenetic tree of Nemacheilidae, including all 471 analysed nemacheilid specimens, reconstructed in MrBayes based on six loci. The topologies of BI and ML trees were congruent. The values at the basal nodes correspond to Bayesian posterior probabilities and ML bootstrap supports, respectively. Only the ingroup is shown.

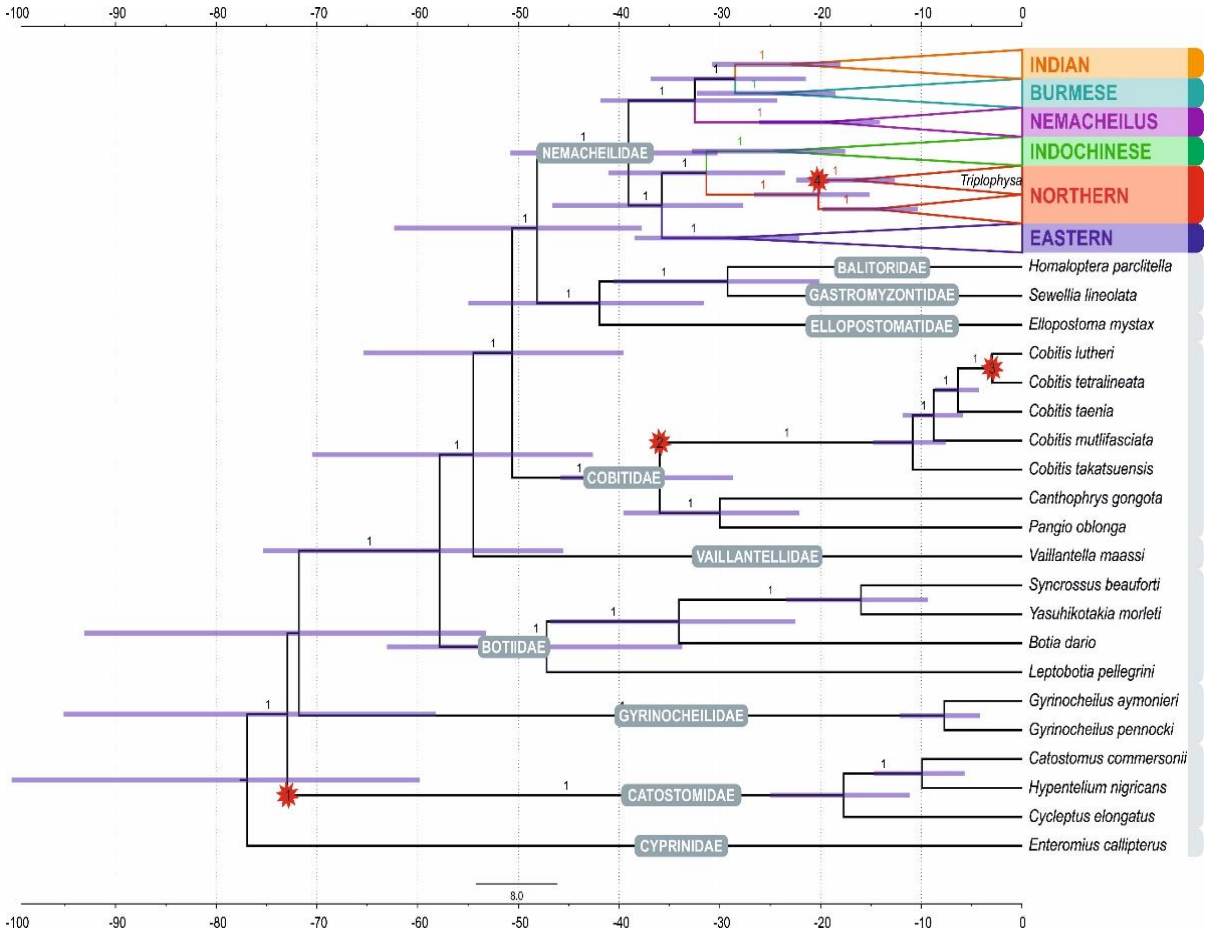

Fig. 2. Divergence time estimation resulting from Bayesian divergence time analysis of concatenated dataset in BEAST 2: maximum clade credibility (MCC) tree of the whole dataset, with the Nemacheilidae ingroup collapsed into main clades. Red stars indicate calibration points, values at branches represent posterior probabilities (PPs lower than 0.90 not shown) and blue horizontal bars denote 95% HPD. The time scale is in millions of years.

Each major clade exhibited a distinct distribution (Fig. 3). Overlap of ranges occur in the Burmese region and in Indochina.

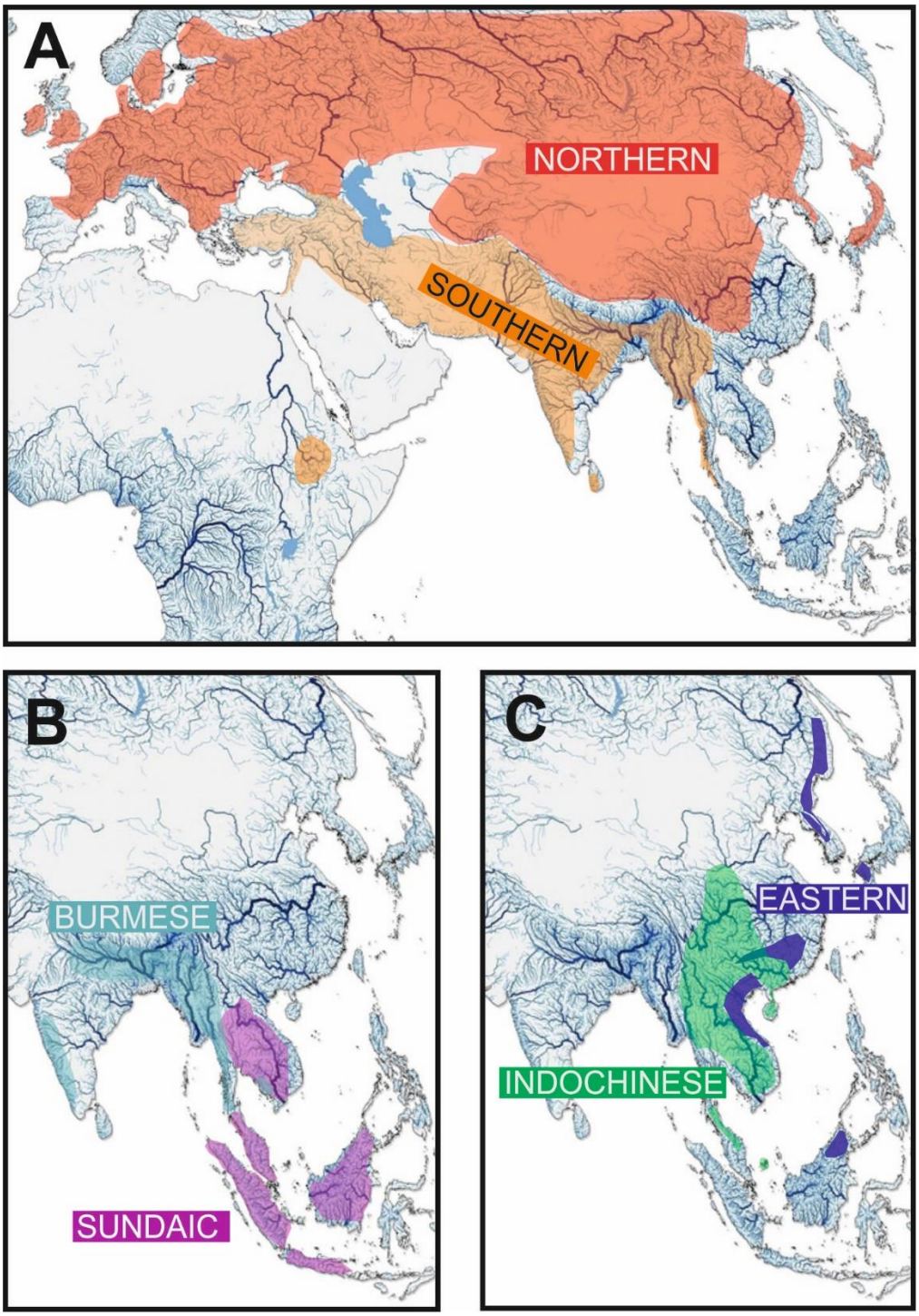

Fig. 3. Geographic distribution of the six major clades of Nemacheilidae.

The most widely distributed is the **‘Northern Clade’** (Fig. 3A), which inhabits the northern parts of Asia and most of Europe from Japan to Spain and southwards to Yunnan. The **‘Southern Clade’** (Fig. 3A) has the second largest distribution and inhabits the Indian subcontinent, the Burmese region and West Asia from the Salween River to southeast Europe; isolated species are found also in Indochina and East Africa (Ethiopia). Another clade is the **‘Burmese Clade’** (Fig. 3B) with a continuous distribution from western Thailand to Northeast India, plus isolated species in the Western Ghats of India and in eastern Thailand and Cambodia. The **‘Sundaic Clade’** (Fig. 3B) includes only the species of the genus *Nemacheilus* and is distributed across Sundaland (the Great Sunda Islands Borneo, Sumatra and Java and the Malay Peninsula) and in the Indochinese rivers draining to the Gulf of Thailand (Mekong, Mae Khlong and Chao Phraya). The **‘Eastern Clade’** (Fig. 3C) is found along the eastern margin of Asia from the Russian Far East to eastern Borneo. Its disjunct distribution consists of a single species in northeast Borneo, the majority of genera and species in northern Vietnam and southeast China and a single genus on the Korean Peninsula, the Japanese Archipelago, northeast China and the Russian Far East.

The sixth clade (**‘Indochinese Clade’**, Fig. 3C) has a continuous distribution throughout Thailand, Laos, Cambodia, Vietnam, central Myanmar and southern China, as well as isolated species in the upper/middle Yangtze and on Tioman Island (Malaysia). The distribution areas of the six major clades are not exclusive, but show little overlap in the cases of Northern, Indochinese and Southern Clades, while the Sundaic Clade shares the northern half of its distribution area with the Indochinese

Clade and the Eastern Clade even shares its northern part of distribution with the Northern Clade, the middle part with the Indochinese Clade and the southernmost point of occurrence with the Sundaic Clade.

Analyses of the concatenated dataset as well as ASTRAL analysis inferring a species tree from single gene trees revealed a basal dichotomy in the family Nemacheilidae (Fig. 1,2,4). The one branch consists of the Eastern Clade as sister to the pair Indochinese plus Northern Clade. The second branch is made of the Sundaic Clade as sister to the pair Burmese and Southern Clade. All basal nodes and most of tip nodes are supported by high statistical supports in all analyses.

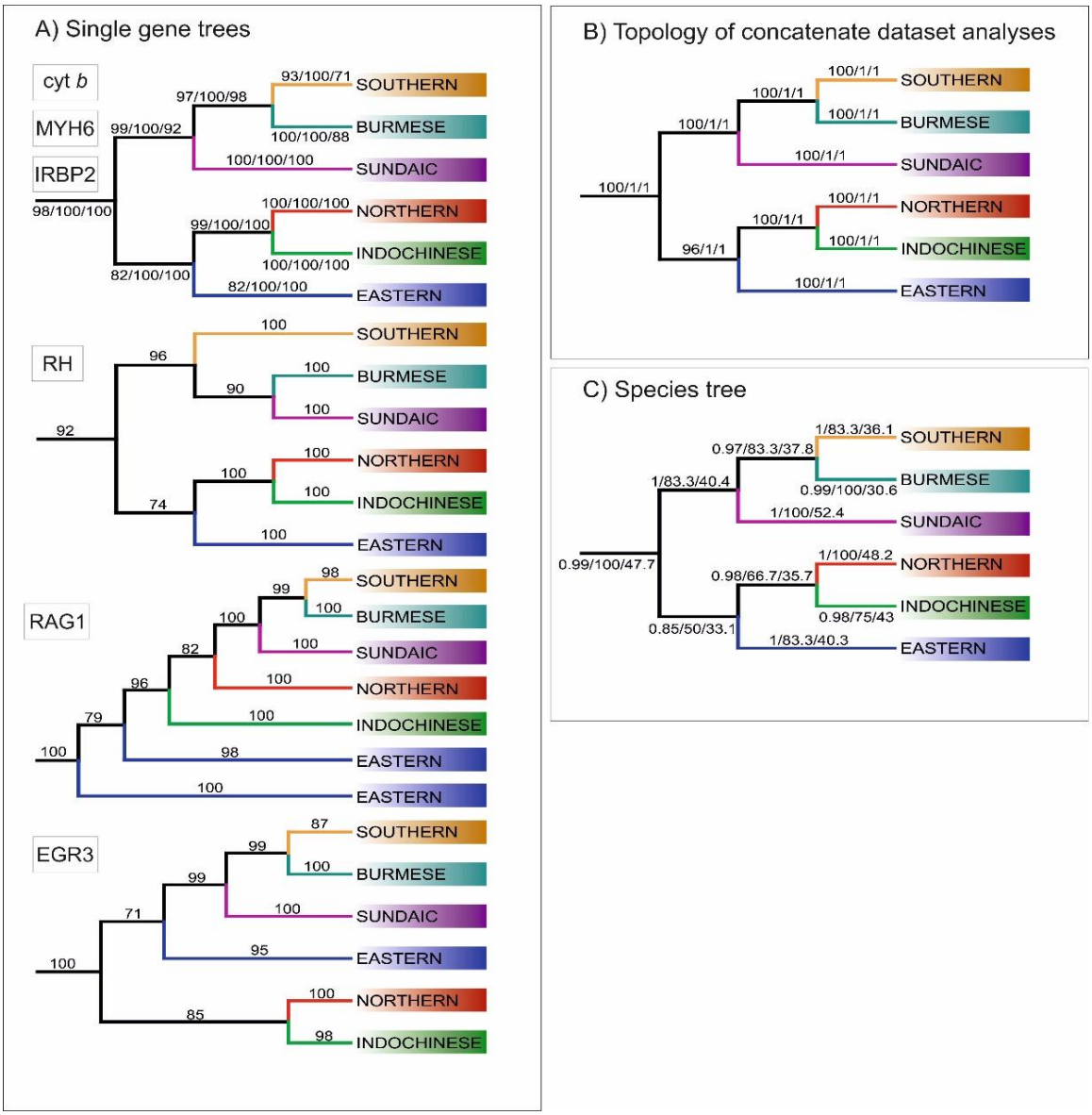

Fig. 4. Topologies of main clades derived from various analyses. A) Topologies recovered by ML analyses of single gene trees, with values at branches indicating bootstrap supports. Topologies congruent to the concatenated data-derived as well as species tree is revealed by Cyt b, MYH6 and IRBP2. Three slightly different topologies were derived from RH, EGR3 and RAG1 B) Topology obtained from analyses of concatenate dataset, the values at the branches correspond to ML/MrBayes PP/BEAST PP supports, respectively. C) Topology inferred by ASTRAL-III using the unrooted ML single gene trees as input. The values at the branches correspond to support values/gCF/sCF.

Divergence times

The ages of the genealogic events were determined using three fossil records and one geological event as calibration points. The results indicate that Nemacheilidae shared the last common ancestor with other families of Cobitoidea about 48.5 mya (Fig. 4). The first notable split that separated the family into two big branches took place around 39 mya (for details see Fig. 5).

Biogeographic reconstructions

The biogeographic reconstruction of Nemacheilidae considered 11 geographic regions within Eurasia and northeast Africa. The results show that Nemacheilidae originated in the region of nowadays Indochina and expanded from there in multiple waves. More details are given in Fig. 6.

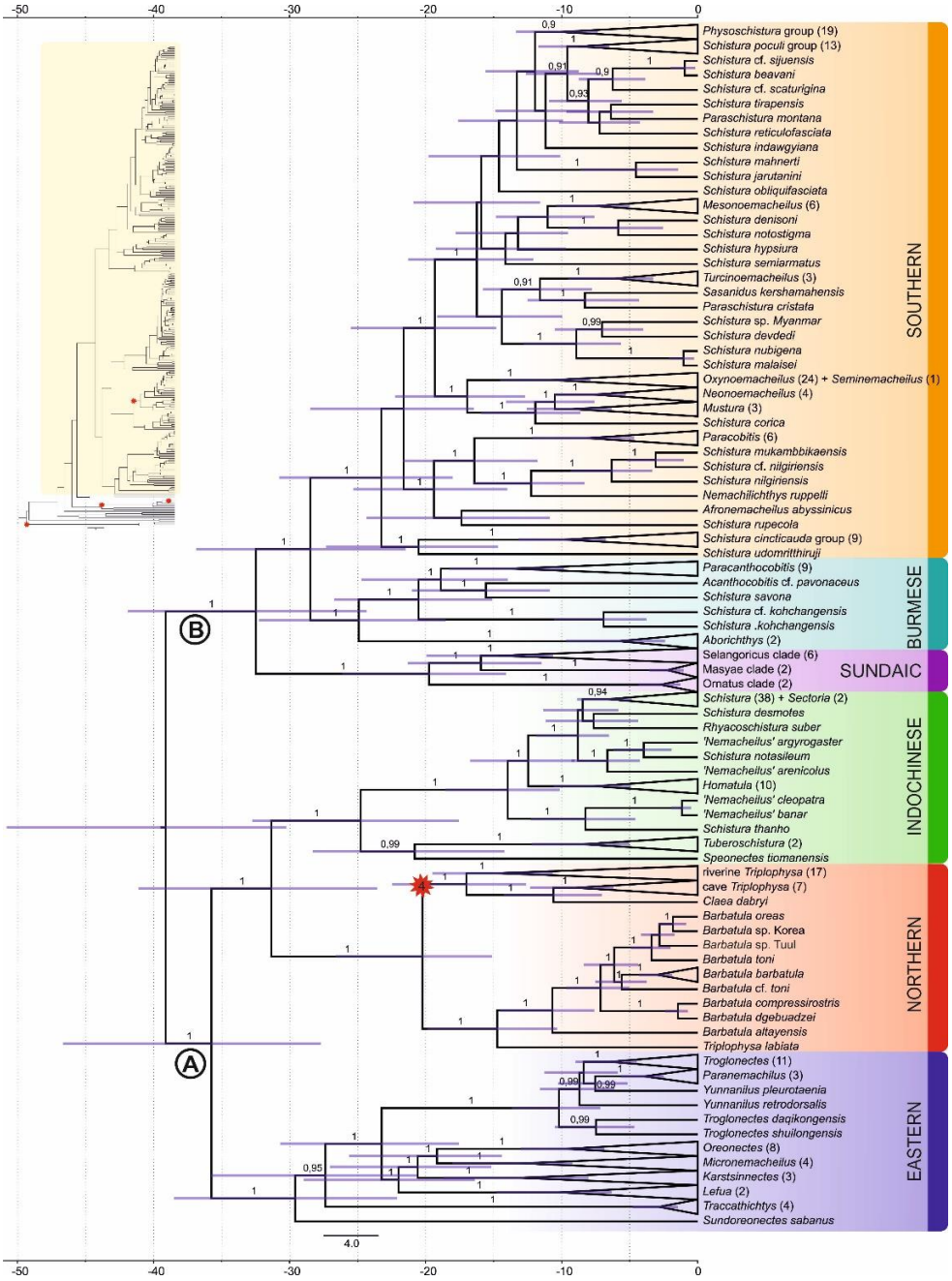

Fig. 5. Divergence time estimation: Ingroup of the maximum clade credibility (MCC) tree resulting from Bayesian divergence time analysis of concatenated dataset in BEAST 2. The red star indicates internal calibration point, the values at the nodes represent posterior probabilities (PPs lower than 0.90 not shown), and the blue bars relevant 95% HPD. The time scale is in millions of years. Inset in top left corner shows complete tree: Nemacheilidae is highlighted in yellow, while the outgroup is not highlighted; all calibration points are indicated by red stars.

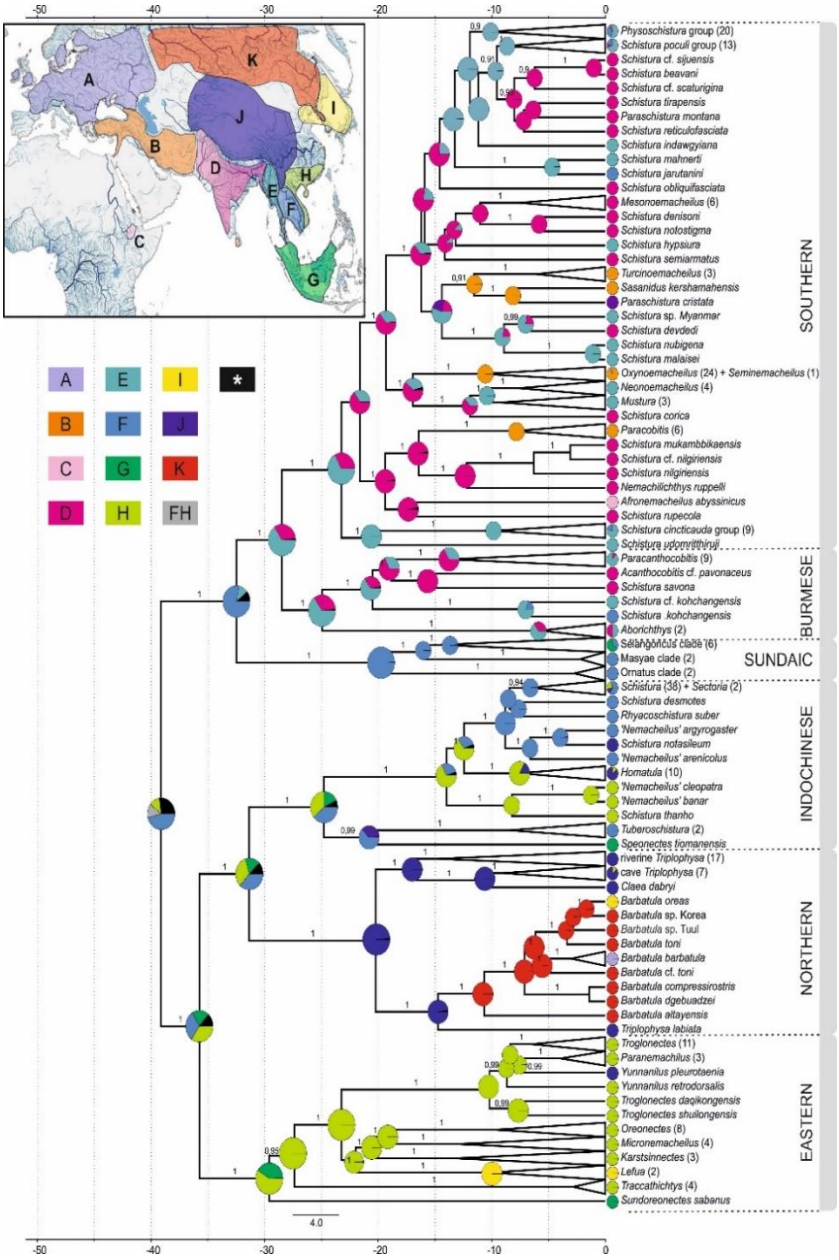

Fig. 6. Reconstruction of the biogeographical history of Nemacheilidae. The inset map in top left corner shows the defined biogeographical regions of Eurasia recognised in the analysis; below the map the colour – region code for the main tree. Grey colour indicates combination of two regions as ancestral (FH); black colour indicates ancestral ranges identified with likelihood < 10% . Main tree: Ancestral range reconstruction with use of DEC+J model based on the phylogeny derived from BEAST2. Pie charts at the nodes indicate relative likelihood of ancestral ranges of most recent common ancestors (MRCA), while the current distribution of taxa is indicated at the tips.

Discussion

The evolutionary history of Nemacheilidae (Fig. 7)

Early Eocene (56 – 48 mya) - the origin of Nemacheilidae (Fig. 8A)

The family Nemacheilidae shared the last common ancestor with the other Cypriniformes about 48.5 mya (Fig. 2), and our biogeographic analysis identified the region of nowadays Indochina as most likely place of origin of Nemacheilidae (Fig. 6). During the early Eocene, Southeast Asia experienced a warm and perhumid climate, characterised by both highlands and lowlands with numerous rivers (Morley 2018), which must have been ideal conditions for stone loaches.

Middle to late Eocene (48 – 34 mya) – first range expansions and formation of the first major clades (Fig. 8B,C)

The first detectable cladogenetic event within the family occurred about 39 mya and separated a lineage formed by the Eastern, Northern and Indochinese Clades (Branch A in Fig. 5) from a lineage including the Sundaic, Burmese and Southern Clades (Branch B). Our biogeographic analysis of the dataset revealed Indochina as most parsimony area of the first cladogenetic event; and consequently as region of origin for branch A as well as branch B.

The Eastern Clade was the first of the six present major clades to form: it separated about 35.8 mya from the common ancestor of the Indochinese and Northern Clades, either in the region of Indochina or Vietnam-south China. Taking into consideration its present-day distribution (Fig. 3) we assume that the young

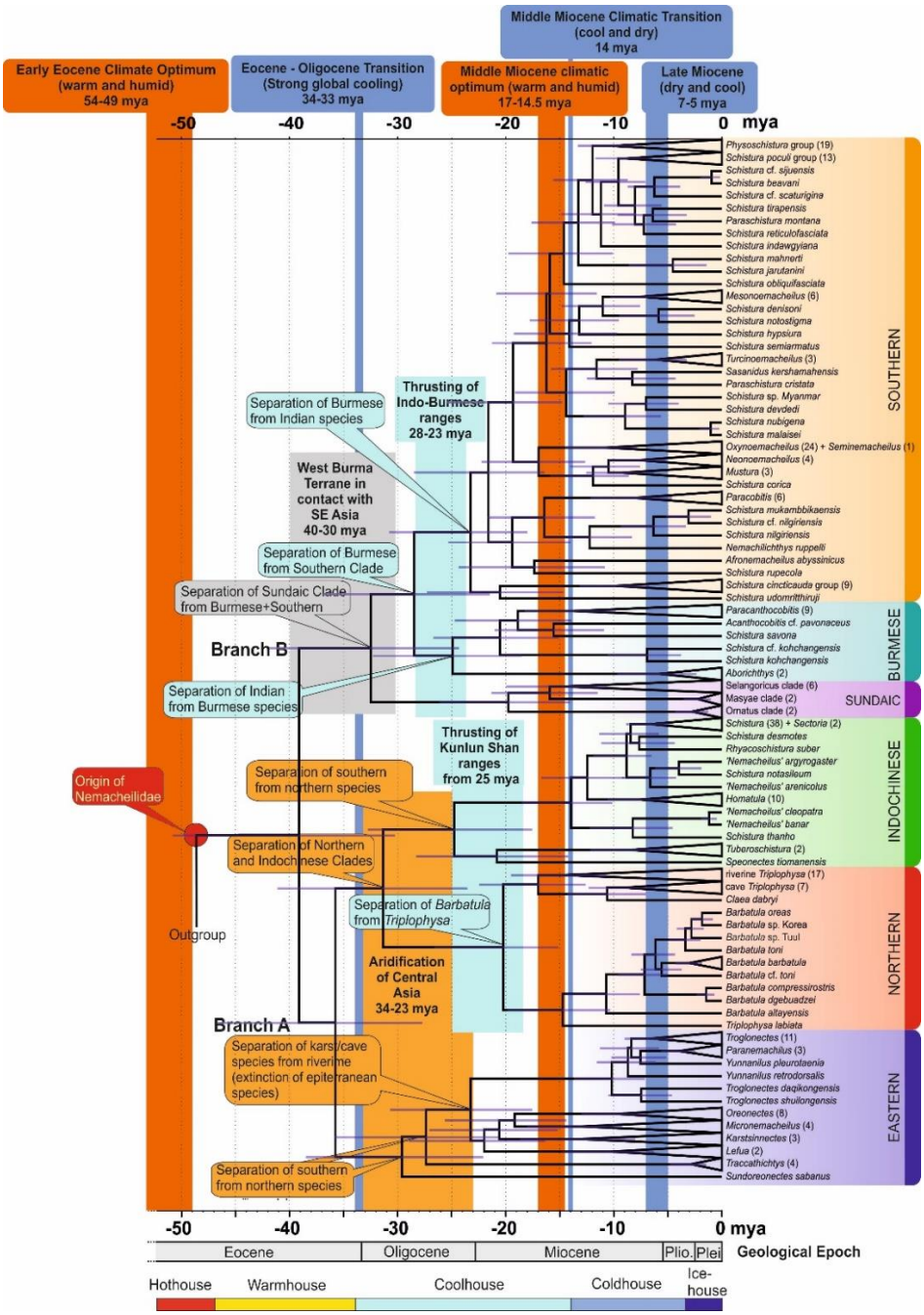

Fig. 7. Time tree of the evolutionary history of Nemacheilidae: The figure presents the evolutionary history of Nemacheildae, highlighting the dating of key geological or climatic key paleo-events that might have significantly impacted their evolution. Orange bars represent exceptionally warm periods, blue bars denote cold periods. Simple boxes give time span of specific geological or climatic event. For detailed explanations of these events and their impact on nemacheilid evolution refer to text.

Eastern Clade spread mainly along the eastern coastline of Asia southwards to Borneo and northwards to northeast China. Geologic data support this hypothesis: During the Eocene, Asia was much smaller than today and had a rather flat relief with old mountains mainly along its eastern coast due to the collision with the Pacific Plate since 190 mya (Seton et al., 2012; Wang, 2004), while the upfolding of east-west mountain ridges had just started. The generally warm and humid climate during Eocene (Morley 2018; Westerhold et al. 2020) promoted the range expansion of the Eastern Clade, while the ancient eastern mountain ranges directed the range expansion. It can be assumed that shortly after the range expansion the distribution of the Eastern Clade was more or less continuous and not separated into several disjunct areas as nowadays.

The ancestral Indochinese + Northern Clades also spread northwards, but their present-day distribution (Fig. 3) suggests that they took a route through Central Indochina and China. Most likely, this first geographic expansion led the ancestral Indochinese+Northern Clades northward to at least the Tibetan Protoplateau, which during Eocene epoch had its northern boundary in the region of the Tanggula Shan (Wang et al., 2008). The presence of the two protoclades on the early Tibetan Plateau is indicated by the presence of some of their most basal members in the Yangtze basin and Yunnan: the genus *Homatula* for the Indochinese Clade and several species of *Triplophysa* for the Northern Clade (Figs. 1,5).

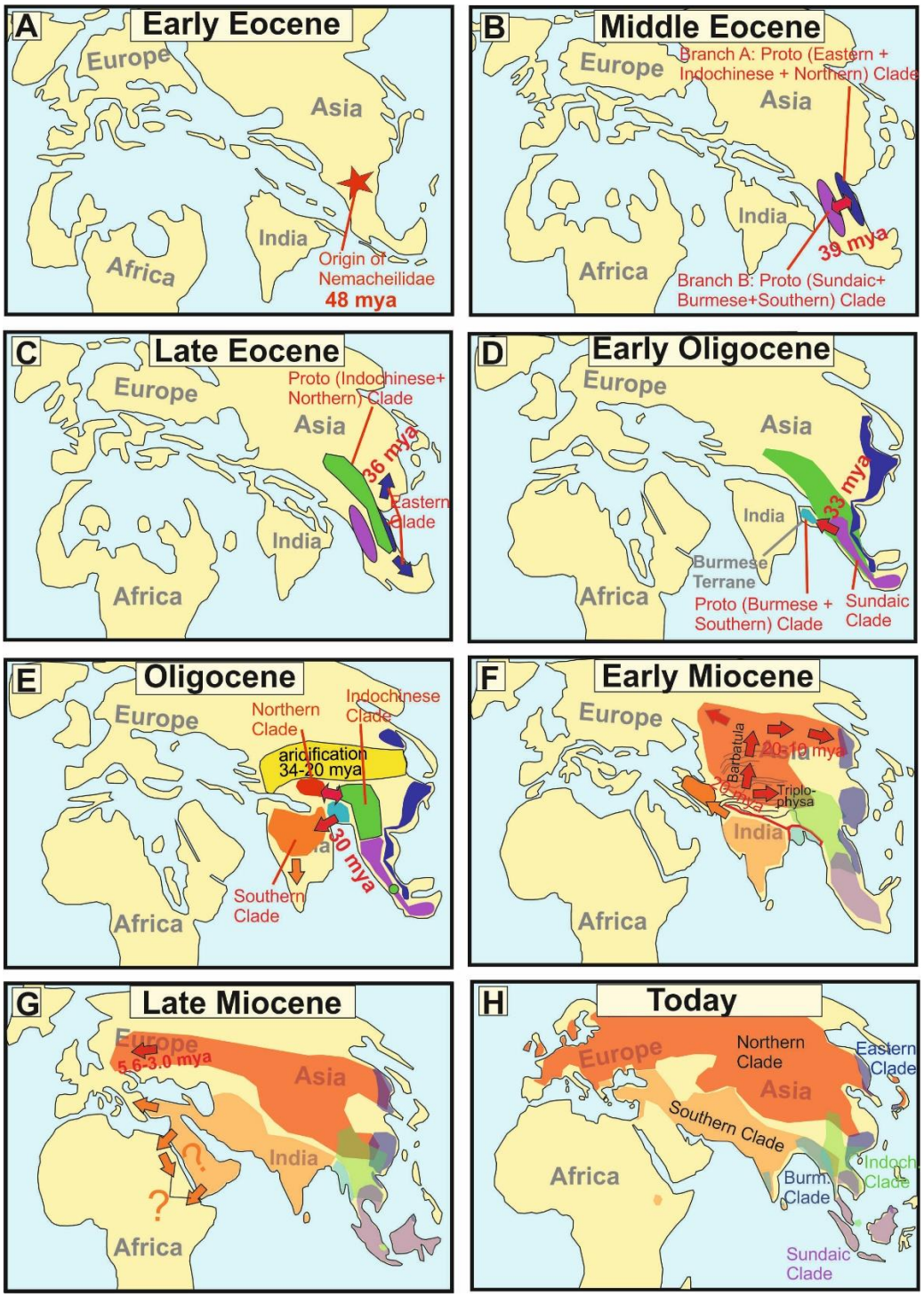

Fig. 8. Series of paleomaps visualising the geographical and chronological aspects of the main events during the evolutionary history of the freshwater fish family Nemacheilidae across Eurasia. A red star marks the point of origin of Nemacheilidae, arrows indicate dispersal events.

Oligocene (34 – 23 mya) – range expansions, extinctions and the formation of the remaining major clades (Fig. 8D,E)

The Eocene - Oligocene transition brought a period of significant global cooling (Hutchinson et al 2021) as well as a change in the precipitation regime of Central Asia (Clift & Webb 2018; Ye et al. 2022) due to the ongoing uplift of the Himalayan Mountains (Ding et al. 2017). A substantial decrease of rainfall in Central Asia caused an aridification from 34 – 23 mya (Bosboom et al. 2014) extending across nearly all of Oligocene Asia from the western to the eastern coast (Wang, 2004). The distribution area of the Eastern Clade became fragmented during this period (Fig. 3).

The Central Asian arid zone also split the Indochinese – Northern protoclade into two part that evolved into two separate major clades, the Indochinese Clade and the Northern Clade. Moreover, the distribution area of the Indochinese Clade was split and separated the southernmost branch (*Speonectes* and *Tuberoschistura*) from the northern branch. The latter presently inhabits all of Indochina and southern China including the middle Yangtze basin (Fig. 3), indicating that the Oligocene refuge of the northern branch of the Indochinese Clade was located southeast of the Tibetan Plateau. In contrast, the early Northern Clade found its refuge further north on the Tibetan Protoplateau, the only region that can explain the further history and the present distribution of the clade. By late Oligocene, the climate in Central Asia returned to a warmer and moister state (Zachos et al. 2001) and the eastern Kunlun Shan Mountains rapidly thrust upward as an expansion of the northern Tibetan Plateau (Li et al. 2021). These favourable conditions coincided with a major split

within the Northern Clade at 20 mya (Fig. 5), when the proto-*Barbatula* clade colonised the Kunlun Mountains, while the proto *Triplophysa* branch found its main distribution rather east of the Tibetan Plateau.

Different geologic events drove the evolution of branch B: the common ancestor of the Burmese and Southern Clades split at 32.5 mya in Indochina from the Sundaic Clade. In contrast to the general trend among Nemacheilidae, the species of the Sundaic Clade (genus *Nemacheilus*) prefer sandy bottom over gravel bottom, making lowlands regions of Sundaland and Indochina their ideal habitat. There are no indications that the Sundaic Clade ever left the region of present-day Southeast Asia.

The separation of the ancestral Burmese and Southern Clades from the Sundaic Clade occurred because the former left Southeast Asia by colonising the West Burma Terrane, a microplate that was pushed northward by the Indian plate (Morley et al. 2021) and made temporary contact with Sundaland around Eocene-early Oligocene (Westerweel et al. 2019). Around 30 mya, it occasionally made contact with northeast India (Morley et al. 2021), allowing fishes from the West Burma Terrane to colonise the Indian subcontinent. During the Oligocene, the Indian plate and the West Burma Terrane both collided with mainland Asia. The former presently forms the Indian subcontinent, the later Western Burma (Westerweel et al. 2020). Their parallel collision with mainland Asia caused the uplift of the north-south directed Indo-Burmese mountain range (Morley et al. 2020), providing a physical barrier between the Brahmaputra basin on the Indian side from the Chindwin-

Irrawaddy basin on the Burmese side, promoting the separation of the two faunas into the Burmese Clade and the Southern Clade.

Miocene (23 – 5.3 mya) – rapid diversification (Fig. 8F,G)

The Miocene is generally an epoch of cooling, with temperatures decreasing about 5.5º C to conditions similar to present day (Zachos et al. 2001). But temperatures also underwent strong fluctuations, leading to exceptionally warm periods like the Middle Miocene Climatic Optimum (17 – 14.5 mya) as well as to drastic cooling events like the Middle Miocene Climatic transition (14 mya) (Morley 2018). Additionally, the Asian monsoon regime strengthened from the early Miocene (Clift & Webb 2018), increasing precipitation and altering the distribution of climatic regions across Asia (Sun & Wang 2005). Moreover, during the Miocene the Himalayan Mountains experienced their main uplift (Ding et al. 2017) and the upfolding area of Central Asia mountain ranges expanded northwards, giving rise to the Tian Shan and Altai mountains (Nissen et al 2009; Liu et al 2023).

During this complex geological and climatic scenario, the fish family Nemacheilidae underwent a massive diversification. In our phylogenetic hypothesis the family comprised 16 lineages at the beginning of Miocene and 177 lineages by the end of the epoch. The radiation occurred across all six major clades, albeit to a lesser extent in the Eastern Clade. Interestingly, it manifested similarly in the region of the Indian monsoon and the East Asian monsoon. In both regions, major radiations occurred during the Middle Miocene Climatic Optimum, including the radiation of the *Barbatula* lineage in the Northern Clade, of the Indochinese Clade,

of all *Nemacheilus* except *N*. *binotatus* and *N*. *ornatus* and of six branches in the Southern Clade. It appears that under increased temperature and precipitation freshwater fishes flourished, across all of Asia and under different monsoon systems.

One of the radiations that began during the Middle Miocene Climate Optimum involves *Afronemacheilus*, the sole nemacheilid genus found in Africa (Prokofiev & Golubtsov 2013). Our results confirm that the ancestral *Afronemacheilus* separated from the Southern Clade about 18 - 17 mya. It could have utilised two potential pathways to Africa: one across the Arabic Peninsula and via the southern Danakil Isthmus, a broad landbridge that stretched from Djibouti to Aden from late Miocene to Pliocene (Bosworth et al. 2005; Steward & Murray 2017). The second pathway would lead through the Levant and via Sinai into the Nile ('*Gomphotherium* landbridge' Harzhauser et al 2007), and subsequently upstream into the Ethiopian highlands. Unfortunately, the nearly complete extinction of freshwater fishes from the Arabic Peninsula and from the Nile during Pleistocene aridification (Kotwicki & Salaimani 2009; Leplongeon 2021) complicates the reconstruction of its pathway to Africa.

In the Northern Clade, the *Triplophysa* lineage flourished during the Miocene. Its present wide distribution in southern and Central China suggests that it expanded from its Oligocene refuge on the eastern Part of the Tibetan Plateau in an eastern direction (Fig. 3). In contrast, the *Barbatula* branch expanded from its refuge on the western Tibetan Plateau northwards, traversing the uplifting Tian Shan and Altai mountains. This expansion can be traced from the geographic position of the most basal species (*T. labiata* -Tian Shan, *B. altayensis* – Altai), and then eastwards (*B.*

compressirostris + *D*. *dzebuadzei* – west Mongolia, *B.* cf. *toni* – east Mongolia; tip species in Korea (*B.* indet Korea) and Japan (*B. oreas*).

During late Miocene, *Barbatula* also expanded westwards through Siberia and colonised Europe between 5.6 mya (separation of the European taxa from the Mongolian sister taxon) and 3.0 mya (oldest split within European *Barbatula*). During this cool and dry period, first glaciations occurred on the northern hemisphere (Zachos et al. 2001), and in Siberia the mean temperature of the coldest month dropped below 0º for the first time (Popova et al. 2012). Freezing of the northern margin of Eurasia impeded the Siberian rivers (which flow from south to north) from discharging their water into the Northern Ocean and produce extensive wetlands on the shallow relief of Siberia. These wetlands served as pathways for freshwater fishes from East Asia to European river systems during Pleistocene (Kalous et al. 2012), and we assume that the same mechanism brought *Barbatula* to Europe during Pliocene.

Pliocene and Pleistocene (5.3 – 0.01 mya) - Ice ages

During Pliocene and Pleistocene global cooling continued until massive glaciations repeatedly covered the north of Eurasia from early Pliocene onwards (de Schepper et al. 2014). However, the Pliocene also brought a much stronger seasonality to Eurasia, especially in the form of cold winters (Shen et al. 2018). Despite these significant changes in climatic conditions, the evolution of Nemacheilidae seems not to have experienced any dramatic negative impact, but reveals mainly local speciation events (e.g. in the genera *Traccatichthys* and *Barbatula*). We know from

more detailed studies on Nemacheilidae (Bohlen et al 2020a,b; Šlechtová et al. 2021) that during Pliocene and Pleistocene also geographic shifts as well as expansions and disappearances occurred, but since these happened on rather local scale they were too insignificant to reflect in the present intercontinental dataset.

Conclusions

- We reconstruct the evolutionary history of the Eurasian fauna during most of Cenozoic era on the example of the freshwater fish family Nemacheilidae. The extensive dataset (471 specimens, 279 species, 6 genes) from across Eurasia and the low dispersal capacity of the model resulted in high resolution of the phylogenetical and biogeographic analysis.
- Molecular phylogeny uncovered six major clades within the family. Dating of cladogenetic events and ancestral range estimation traced the origin of Nemacheilidae to Indochina around 48 million years ago.
- Major expansions were facilitated by tectonic connections, favourable climatic conditions, and orogenic processes. Conversely, aridification emerged as the primary cause of extinction events.
- Our study represents the first comprehensive and holistic reconstruction of the evolution of Eurasian freshwater biodiversity on a continental scale and through deep geological time.

Methods

Sampling and Laboratory procedures

471 samples of more than 250 species from 37 described genera of the family Nemacheilidae were examined, including the set of sequences of 364 specimens analysed in our laboratory and sequences of 107 specimens obtained from GenBank. Specimens used for the present study were fixed and stored in 96% ethanol. For more details about samples, sampling sites and GenBank accession numbers see Supplementary material Table 1.

Total genomic DNA was isolated using the DNeasy Blood & Tissue kit (Qiagen) following the manufacturer's instructions. One mitochondrial gene (cytochrome *b*) and five nuclear genes (RAG1, IRBP2, MYH6, RH1 and EGR3) were selected. For list of primers see Supplementary material Table 2, details about PCRs settings are described in Dvořák et al., 2022; Chen et al., 2003 and Chen et al., 2008.

Sequencing of the PCR products was performed in Laboratory of Fish Genetics on ABI Prism 3130 GA or via sequencing service in Macrogen Europe BV (Amsterdam, Netherlands).

Phylogenetic analyses

Chromatograms were checked and assembled in the SeqMan II module of the DNA Star software package (LASERGENE). Single gene alignments were done in BioEdit (Hall, 1999) with use of ClustalW (Larkin et al., 2007) multiple alignment algorithm. TheThe datasets were concatenated in PhyloSuite v1.2.2 (Zhang et al., 2020).

The best-fit substitution models and partitioning schemes (Supplementary material Table 3) were estimated using Partition Finder 2 (Lanfear et al., 2016) implemented in PhyloSuite 1.2.2 based on the corrected Akaike Information Criterion (AICc).

The 471 specimen phylogenetic trees were inferred from six loci concatenated dataset using the maximum likelihood (ML) and Bayesian inference (BI). The ML analyses were performed using IQ-TREE (Nguyen et al., 2015) implemented in PhyloSuite. The best-fit evolutionary model for each codon partition was automatically determined by ModelFinder (Kalyaanamoorthy, et al. 2017). The node support values were obtained with 5000 ultrafast bootstrap replicates (UFBoot) (Hoang et al., 2018). For the BI analyses we used MrBayes 3.2.7a (Ronquist & Huelsenbeck, 2003) on CIPRES Science Gateway (Miller et al., 2010). The datasets were partitioned into genes and codon positions and analyses were performed in two parallel runs of 10-20 million generations with 8 Metropolis Coupled Markov Chains Monte Carlo (MCMCMC). The relative burnin of 25% was used and from the remaining trees a 50% majority rule consensus trees were constructed.

For reconstructing of the species tree we used the Accurate Species TRee ALgorithm (ASTRAL III) (Zhang et al., 2018). For ASTRAL we used unrooted single gene ML trees reconstructed in IQ-TREE implemented in PhyloSuite. We have used IQ-TREE 2 (Minh at al., 2020) to calculate gene concordance factor (gCF, indicating the percentage of decisive gene trees containing particular branch) and site concordance factor (sCF, indicating the percentage of decisive alignment sites that support a branch in the reference tree) for every branch in the ASTRAL species tree.

Distribution maps in Fig. 2 were designed using HYDROSHEDS (Lehner & Grill 2013).

Divergence time estimations and ancestral range reconstruction

The ages of cladogenetic events were estimated in BEAST 2.6.4 (Bouckaert et al., 2014) via CIPRES Science Gateway with use of four calibration points. The first calibration point is based on the oldest known fossil of the family Catostomidae, *Wilsonium brevipinne*, from early Eocene (Liu, 2021), approximately 56-48 my old. The second calibration point is derived from the only known nemacheilid fossil record, *Triplophysa opinata* from Kyrgyzstan from middle-upper Miocene (16.0 to 5.3 mya) (Prokofiev, 2007; Böhme and Ilg, 2003). Third calibration point is based on the oldest known fossil of the genus *Cobitis*, *C. naningensis*, from early to middle Oligocene in southern China*,* 34-28 my old (Chen et al., 2015). The fourth calibration point, based on the river history of the southern Korean Peninsula, dates the separation between the species *Cobitis tetralineata* and *C. lutheri* to 2.5-3.5 my (Kwan et al. 2014). For the fossil-based calibration points we have used a fossil calibration prior implemented in CladeAge (Matschiner et al., 2017), the fourth calibration point was set to a uniform prior (2.5 – 3.5). The calibration points are depicted in Figs. 2 and 5.

For the final analyses, the partitions were unlinked and assigned the estimated evolutionary models. We used relaxed lognormal molecular clock and birth-death prior. Given the large and complex nature of our dataset, and in light of several preliminary analyses where MCMC chains did not provide satisfactory ESSs even after 1 billion iterations, made the decision to streamline the dataset by retaining only one specimen per species. To enhance the performance of the analysis, we also implemented parallel tempering using the CoupledMCMC package (Müller & Bouckaert, 2019, 2020). The analysis was configured with four parallel chains of $6x10^8$ generations, with resampling every 1000. Tree and parameter sampling intervals were set to 60.000. The effective sampling sizes (ESS) for all parameters were assessed in Tracer 1.7.1 (Rambaut et al., 2018). A maximum clade credibility (MCC) tree was built in TreeAnnotator 2.6.0 (Rambaut & Drummond, 2010) after discarding the first 25% of trees. The final trees were visualised in FigTree 1.4.4 (Rambaut, 2019). ML and BI were performed with both full as well as the reduced datasets.

The biogeographical analysis was conducted using the BioGeoBEARS package (Matzke, 2013) implemented in RASP 4.0 (Reconstruct Ancestral Stage in Phylogenies, Yu et al., 2015). We set 11 biogeographic regions according to drainage areas separated by major mountain ridges (Ural, Caucasus. Himalayas, Tenasserim Ridge, Indo-Burmese Range, Annamite Cordilliera, Balkan, Hindukush) or saltwaser straits (Red Sea) (see Fig. 4A). For the analysis, we utilized the final MCC tree and 100 post burnin trees from the previous BEAST analysis. A maximum of 2-unit areas was allowed to be present in every reconstructed ancestral range. The comparison of six biogeographic models (DEC, DEC+J, DIVALIKE,

DIVALIKE+J, BAYAREALIKE, BAYAREALIKE+J) suggested that the DEC+J is the best-suited model for the given dataset (as indicated by AICc weight value, Supplementary material Table 4). Likelihood Ratio Test (LRT) p-values, comparing models with and without the J factor, indicated that the addition of the J factor significantly influences the model likelihood. Considering recent criticisms of DEC and DEC+J (Ree & Sanmartin, 2018), we opted to conduct the analysis not only with DEC+J but also with other +J models. Comparison of the results from all applied models revealed only minimal differences.

References

Andreyenkova, N. G. et al. Phylogeography and demographic history of the black kite *Milvus migrans*, a widespread raptor in Eurasia, Australia and Africa. *J Avian Biol.* (2021).

Antonelli, A. et al. Geological and climatic influences on mountain biodiversity. *Nat. Geosci.* **11**, 718-725 (2018).

Ballarin, F. & S. Q. Li. Diversification in tropics and subtropics following the mid-Miocene climate change: a case study of the spider genus *Nesticella*. *Glob. Chang. Biol.* **24** (2), e577–e591 (2018).

Bănărescu, P. *Zoogeography of Fresh Waters, Vol. 2: Distribution and Dispersal of Freshwater Animals in North America and Eurasia.* AULA, Wiesbaden 1992.

Bohlen, J., Dvořák, T., Šlechta, V. & V. Šlechtová. Sea water shaping the freshwater biota: Hidden diversity and biogeographic history in the Paracanthocobitis zonalternans species complex (Teleostei: Nemacheilidae) in western Southeast Asia. *Mol. Phylogenet. Evol*. **148**, 106806 (2020a).

Bohlen, J., Dvořák, T., Šlechta, V. & V. Šlechtová. Resolving an unnoticed diversity within the Schistura robertsi species complex (Teleostei: Nemacheilidae) using molecules and morphology. *Mol. Phylogenet. Evol*. **151**, 106894 (2020b).

Böhme, M. & A. Ilg. 2003. fosFARbase, www.wahre-staerke.com/ (accessed 27. November 2023).

Bosboom, R. et al. *Aridification in continental Asia after the Middle Eocene Climatic Optimum (MECO). Earth and Planet. Sci. Lett.* ***389****, 34-42 (*2014*).*

Bosworth et al. The Red Sea and Gulf of Aden basins. *J. Afr. Earth Sci*. **43,** 334-378 (2005).

Bouckaert, R. et al. BEAST 2: A Software Platform for Bayesian Evolutionary Analysis. *PLoS Comput. Biol*. **10**, e1003537 (2014).

Chen W.-J., Bonillo C. & G. Lecointre. Repeatability of clades as criterion of reliability: a case study for molecular phylogeny of Acanthomorpha (Teleostei) with larger number of taxa. *Mol. Phylogenet. Evol.* **26**, 262-288 (2003).

Chen, G.-J. et al. First fossil cobitid (Teleostei: Cypriniformes) from Early-Middle Oligocene deposits of South China. *Vert. PalAs*. **53** (4), 299–*309 (*2015).

Chen, W.-J., Miya, M., Saitoh, K., & R. L. Mayden. Phylogenetic utility of two existing and four novel nuclear gene loci in reconstructing Tree of Life of ray-finned fishes: The order Cypriniformes (Ostariophysi) as a case study. *Gene* **423**, 125-134 (2008).

Chu, S.-L. & Y.-R. Chen. A new blind cobitid fish (Pisces, Cypriniformes) from subterranean waters in Yunnan, China. *Acta Zool. Sin.* **25** (3), 285-287 (1979).

Clift, P.D. & A.A.G. Webb. A history of the Asian monsoon and its interactions with solid Earth tectonics in Cenozoic South Asia. P.J. Treloar, M.P. Searle (Eds.), Himalayan Tectonics: A Modern Synthesis, London, Special Publications, Geological Society (2018).

De Schepper, S., Gibbard, P. L., Salzmann, U. & J. Ehlers. A global synthesis of the marine and terrestrial evidence for glaciation during the Pliocene Epoch. *Earth Sci. Rev.* **135**, 83-102 (2014).

Delić, T., Stoch, F., Borko, Š., Flot, J. F. & C. Fišer. How did subterranean amphipods cross the Adriatic Sea? Phylogenetic evidence for dispersal–vicariance interplay mediated by marine regression–transgression cycles. *J. Biogeogr.* **47** (9), 1875−1887 (2020).

Deng, T., Wu, F. X., Zhou, Z. K. & T. Su. Tibetan Plateau: an evolutionary junction for the history of modern biodiversity. *Sci. China Earth Sci.* **63** (2), 172−187 (2020).

Ding, L. et al. Quantifying the rise of the Himalaya orogen and implications for the South Asian monsoon. *Geology* **45** (3), 215–218. (2017).

Dvořák, T., Šlechtová, V. & Bohlen, J. Using species groups to approach the large and taxonomically unresolved freshwater fish family Nemacheilidae (Teleostei: Cypriniformes). *Biology* ***11***, 175 (2022a).

Feduccia, A. Explosive evolution in Tertiary birds and mammals. *Science.* **267** (5198), 637–638 (1995).

Friedman, M. Explosive morphological diversification of spiny-finned teleost fishes in the aftermath of the end-Cretaceous extinction. *Proc. Royal Soc. B.* **277** (1688), 1675–1683 (2010).

Fritz, S. A. et al. Twenty-million-year relationship between mammalian diversity and primary productivity. *Proc. Natl Acad. Sci. USA* **113**, 10908–10913 (2016).

Gu, Q. et al. Phylogeographic relationships and the evolutionary history of the *Carassius auratus* complex with a newly born homodiploid raw fish (2nNCRC). *BMC Genom.* **23**, 242 (2022).

Hall, T. A. BioEdit: a user-friendly biological sequence alignment editor and analysis program for Windows 95/98/NT. *Nucl. Acids. Symp. Ser*. **41**, 95-98 (1999).

Harzhauser et al. Biogeographic responses all around the Oligo-Miocene Tethyan seaway. Zool. Anz. 246, 241-256 (2007)

Hoang, D. T. Chernomor, O., von Haeseler, A., Minh B. Q. **&** L. S. Vinh. UFBoot2: Improving the ultrafast bootstrap approximation. *Mol. Biol. Evol.* **35**, 518–522 (2018).

Hutchinson, D. K. et al. The Eocene–Oligocene transition: a review of marine and terrestrial proxy data, models and model–data comparisons. *Clim. Past* **17**, 269–315 (2021).

Ishii, H. et al. Phylogeography of the stone marten (Martes foina: Mustelidae: Mammalia) in Eurasia, based on a mitochondrial DNA analysis. *Mammal Res.* **68**, 375–381 (2023).

Kahlke, R. D. The origin of Eurasian Mammoth Faunas (*Mammuthus–Coelodonta* Faunal Complex). *Quat. Sci. Rev.* **96**, 32-49 (2014).

Kalous, L., Rylková, K., Petrtýl, M. & J. Bohlen. Hidden diversity within the Prussian carp and designation of a neotype for *Carassius gibelio*. *Ichthyol. Explor. Freshw.* **23**, 11-18 (2012).

Kalyaanamoorthy. S., Minh, B. Q., Wong, T. K. F., von Haeseler, A. & L. S. Jermiin. ModelFinder: fast model selection for accurate phylogenetic estimates. *Nat Methods.* **14** (6), 587–589 (2017).

Kottelat, M. Conspectus Cobitidum: An inventory of the loaches of the world (Teleostei: Cypriniformes: Cobitoidei). *Raf. Bull. Zool*. **26**, 1– 99 (2012).

Kotwicki, V. & Salaimani, Z. Climates of the Arabian Peninsula – past, present, future. *Int. J. Clim. Chang. Strateg. Manag.* **1**, 297-310 (2009).

Kwan, Y. S., Ko, M. H. & Y. J. Won. Genomic replacement of native Cobitis lutheri with introduced C. tetralineata through a hybrid swarm following the artificial connection of river systems. *Ecol. Evol.* **4** (8), 1451-65 (2014).

Lanfear, R., Frandsen, P. B., Wright, A. M., Senfeld, T. & B. Calcott. Partition Finder 2: new methods for selecting partitioned models of evolution for molecular and morphological phylogenetic analyses. *Mol. Biol. Evol*. **34** (3), 772-773 (2016).

Larkin, M. A. et al. Clustal, W & Clustal, X. Version 2.0. *Bioinformatics* **23**, 2947–2948 (2007).

Lehner, B. &, Grill G. Global river hydrography and network routing: baseline data and new approaches to study the world's large river systems. *Hydrological Processes*, 27(15): 2171–2186 (2013).

Leplongeon, A. The main Nile valley at the end of the Pleistocene (28-15 ka): Dispersal corridor or environmental refugium? *Front. Earth Sci.* 8.607183 (2021)

Li, C. et al. Late Oligocene tectonic uplift of the East Kunlun Shan: Expansion of the northeastern Tibetan Plateau. *Geophys. Res. Lett.* **48**, e2020GL091281 (2021).

Liu, J. Redescription of "*Amyzon" brevipinne* and remarks on North American Eocene catostomids (Cypriniformes: Catostomidae)". *J. Syst. Palaeontol.* ***19*** *(9), 1–13 (2021).*

Liu, X. et al. Tectonic uplift of the Tianshan Mountains since Quaternary: evidence from magnetostratigraphy of the Yili Basin, northwestern China. *Int. J. Earth Sci.* **112**, 855–865 (2023).

Matschiner, M. et al. Bayesian node dating based on probabilities of fossil sampling supports trans-Atlantic dispersal of cichlid fishes. *Syst. Biol.* **66**, 3-22 (2017).

Matzke, N. J. Probabilistic Historical Biogeography: New Models for Founder-Event Speciation, Imperfect Detection, and Fossils Allow Improved Accuracy and Model-Testing. *Front. Biogeogr.* **5**, 242–248 (2013).

Mayhew, P. J., Bell, M. A., Benton, T. G. & McGowan, A. J. Biodiversity tracks temperature over time. *Proc. Natl Acad. Sci. USA* **109**, 15141–15145 (2012).

Miller, M. A., Pfeiffer, W. & T. Schwartz. Creating the CIPRES Science gateway for inference of large phylogenetic trees. Proc. Gateway Computing Environments Workshop 2010 pages 1–8, New Orleans, LA, November, 2010.

Minh, B. Q., Hahn, M. & W. R. Lanfear. New methods to calculate concordance factors for phylogenomic datasets. *Mol. Biol. Evol.* **37**, 2727–2733 (2020).

Morley, R. J. Assembly and division of the South and South-East Asian flora in relation to tectonics and climate change. *J. Trop. Ecol.* **34** (4), 209-234 (2018).

Morley, C. K., Naing, T. T., Searle, M. & S. A. Robinson. Structural and tectonic development of the Indo-Burma ranges. *Earth Sci. Rev.* **200**, 102992 (2020).

Morley, R. J. et al. Sequence biostratigraphic framework for the Oligocene to Pliocene of Malaysia: High-frequency depositional cycles driven by polar glaciation. *Palaeogreogr. Palaeoclimatol. Palaeoecol.* **561**, 110058 (2021).

Mudelsee, M., Bickert, T., Lear, C. H. & G. Lohmann. Cenozoic climate changes: A review based on time series analysis of marine benthic $\delta^{18}O$ records. *Rev. Geophysics* **52**, 333-374 (2014).

Müller, N. F. & R. Bouckaert. Adaptive Metropolis-coupled MCMC for BEAST 2. *PeerJ* 16:8:e9473 (2020).

Müller, N. F. & R. Bouckaert. Coupled MCMC in BEAST 2. *bioRxiv* (2019).

Nguyen L.-T., Schmidt, H. A., von Haeseler, A. **&** B. Q. Minh. IQ-TREE: A fast and effective stochastic algorithm for estimating maximum likelihood phylogenies. *Mol. Biol. Evol.* **32**, 268-274 (2015).

Nissen, E., Walker, R., Molor, E., Fattahi, M. & A. Bayasgalan. Late Quaternary rates of uplift and shortening at Baatar Hyarhan (Mongolian Altai) with optically stimulated luminescence. *Geophys. J. Inter.* **177** (1), 259–278 (2009).

Popova, S., Utescher, T., Gromyko, D. Bruch, A. & V. Mosbrugger. Palaeoclimate Evolution in Siberia and the Russian Far East from the Oligocene to Pliocene – Evidence from Fruit and Seed Floras. *Turk. J. Earth Sci.* **21** (2), 315–344 (2012).

Prokofiev, A. M. & A. S. Golubtsov. Revision of the loach genus *Afronemacheilus* (Teleostei: Balitoridae: Nemacheilinae) with description of a new species from the Omo-Turkana basin, Ethiopia. *Ichthyol. Explor. Freshw.* **24** (1), 1-14 (2013).

Prokofiev, A. M. Redescription of a fossil loach Triplophysa opinata (Yakowlew, 1959) from the Miocene of Kirgizia (Balitoridae: Nemacheilinae). J. Ichthyol. **47**, 26–31 (2007).

Rambaut A. 2019. *Figtree version 1.4.4* Available from http://tree.bio.ed.ac.uk/software/figtree.

Rambaut, A. & A. J. Drummond. 2010. TreeAnnotator version 1.6.1 Available from http://beast.bio.ed.ac.uk/TreeAnnotator.

Rambaut, A., Drummond, A. J., Xie, D., Baele, G. & M. A. Suchard. Posterior summarisation in Bayesian phylogenetics using Tracer 1.7. *Syst. Biol*. **67** (5), 901–904 (2018).

Ree, R.H. & I. Sanmartin. Conceptual and statistical problems with the DEC+J model of founder-event speciation and its comparison with DEC via model selection. *J. Biogeogr.* **45** (4), 741–749 (2018).

Ronquist, F. & J. P. Huelsenbeck. MRBAYES 3: Bayesian phylogenetic inference under mixed models. *Bioinformatics* **19**, 1572-1574 (2003).

Saito, T. *et al.* Phylogeography of freshwater planorbid snails reveals diversification patterns in Eurasian continental islands. *BMC Evol. Biol.* **18**, 164 (2018).

Seton, M.et al. Global continental and ocean basin reconstructions since 200 Ma. *Earth Sci. Rev.* **113** (3-4), 212-270 (2012).

Shen, X. et al. Increased seasonality and aridity drove the C4 plant expansion in Central Asia since the Miocene–Pliocene boundary. *Earth Planet. Sci. Lett.* **502**, 74-83 (2018).

Šlechtová, V., Musilová, Z., Tan, H.H., Kottelat, M. & J. Bohlen. One northward, one southward: Contrasting biogeographical history in two benthic freshwater fish genera across Southeast Asia (Teleostei: Cobitoidea: *Nemacheilus*, *Pangio*). *Mol. Phylogenet. Evol*. **161**, 107139 (2021).

Steward, K. M. & A. M. Murray. Biogeographic implications of fossil fishes from the Awash River, Ethiopia. *J. Vertebr. Paleont*. **37,** e1269115 (2017).

Summerhayes, C. P. *Earth's climate evolution*. Wiley Blackwell, 2015. ISBN: 978-1-118-89739-3

Sun, X. & P. Wang. How old is the Asian monsoon system? Palaeobotanical records from China. *Palaeogreogr. Palaeoclimatol. Palaeoecol.* **222**, 181-222 (2005).

Trifonov, V. G., Ivanova, T. P. & D. M. Bachmanov. Recent Mountain Building of the Central Alpine–Himalayan Belt. *Geotectonics* **46** (5), 315–332. (2012).

Wang, C. et al. Constraints on the early uplift history of the Tibetan Plateau. *Proc. Natl Acad. Sci. USA* **105** (13), 4987-4992 (2008).

Wang, P. Cenocoic deformation and the history of sea-land interactions in Asia. In: Clift, P., Wang, P., Kuhnt, W., Hayes, D. (Eds.), Continent-Ocean Interactions in the East Asian Marginal Seas. *Geophys. Monogr. Ser.* **149**, 1-22 (2004).

Westerhold, T. et al. An astronomically dated record of Earth's climate and its predictability over the last 66 million years. *Science* **369** (6509), 1383–1387 (2020).

Westerweel, J. et al. Burma Terrane collision and northward indentation in the Eastern Himalayas recorded in the Eocene-Miocene Chindwin Basin (Myanmar). *Tectonics* **39**, e2020TC006413 (2020).

Westerweel, J. et al. Burma Terrane part of the Trans-Tethyan arc during collision with India according to palaeomagnetic data. *Nat. Geosci.* **12**, 863–868 (2019).

Ye, J. W., Tian, B. & D. Z. Li. Monsoon intensification in EastAsia triggered the evolution of its flora. *Front. Plant. Sci.* **13,** 1046538 (2022).

Yu, Y., Harris, A. J., Blair, C. & X. He. RASP (Reconstruct Ancestral State in Phylogenies): a tool for historic biogeography. *Mol. Phylogenet. Evol*. **87**, 46–49 (2015).

Zachos, J. C., Pagani, M., Sloan, L. C., Thomas, E. & K. Billups. Trends, rhythms, and aberrations in global climate 65 Ma to present. *Science* **292**, 689–693 (2001).

Zhang, C., Rabiee, M., Sayyari, E. & S. Mirarab. ASTRAL-III: polynomial time species tree reconstruction from partially resolved gene trees. BMC Bioinform. **19**, 153 (2018).

Zhang, D. et al. PhyloSuite: an integrated and scalable desktop platform for streamlined molecular sequence data management and evolutionary phylogenetics studies. *Mol Ecol Resour*. **20** (1), 348–355 (2020).

Acknowledgements

VŠ, TD, VŠ and JB would like to thank R. Hoyer, J. Kühne, F.F. Kullander (NRM), Jan Kusznierszz, K. Lim (ZRC), H. Linke, A. Nolte, G. Ott, M. Reichard, I. Seidel, S. Somadee, H.H. Tan (ZRC), T.K. Toe, K. Udomritthiruji, T. Win and U. Wolf for their help with obtaining specimens for this study and Š. Pelikanová for help with laboratory work. VŠ and JB were funded by grants 206/08/0637 and 19-18453S of the Grant Agency of the Czech Republic. BL and AG greatly acknowledge S. Cherenkov for his help in sampling. BL was supported by Russian Science Foundation, grant no. 24-44-20019.

SUPPLEMENTARY INFORMATION

Table S1.

List of analysed samples, their identification, geographical origin, voucher number and GenBank accession numbers for their sequences. Voucher numbers starting with 'A' refer to the collection of IAPG, Liběchov, Czech Republic; 'CMK' numbers refer to the collection of Maurice Kottelat; 'GenBank' refers to sequences from GenBank; 'ZRC' to samples housed in the Lee Kong Chian Natural History Museum, National University of Singapore, Singapore.

Species name	Country	Province	River basin	voucher	Cyt b	RAG 1	IRBP2	MYH6	RH 1	EGR 3
EASTERN CLADE										
Karstsinnectes acridorsalis	China	Guangxi	Pearl	GenBank	ON116515	OP473644	-	OP473686	OP473776	OP473850
Karstsinnectes anophthalmus	China	Guangxi	Pearl	GenBank	ON116506	OP473637	OP473907	OP473664	OP473763	OP473828
Karstsinnectes parvus	China	Guangxi	Pearl	GenBank	ON116520	OP473651	OP473900	OP473693	-	OP473859
Lefua costata	Korea	Gangwon	Cheon Jin Cheon	A1895	PP279919	PP315753	PP280130	PP280341	-	-
				A6942	KP738591	KP738551	KP738511	OL191348	-	PP259693
Lefua torrentis	Japan	Hyogo	Kako	A1050	PP279878	PP315711	PP280091	PP280288	PP259745	-
				A1051	PP279879	PP315712	PP280092	PP280289	PP259747	-
				A1052	PP279880	PP315714	PP280093	PP280291	PP259748	-
Micronemacheilus bailianensis	China	Guangxi	Pearl	GenBank	ON116504	OP473620	OP473876	OP473662	OP473759	OP473825
Micronemacheilus cruciatus	Vietnam	Thua Tien-Hue	Song Bu Lu	A3293	PP279965	PP315801	-	PP280394	PP259847	PP259670
				A3294	PP279966	PP315802	-	PP280395	PP259848	PP259671
Micronemacheilus longibarbatus	China	Guangxi	Pearl	GenBank	ON116508	OP473625	OP473879	OP473666	OP473761	OP473833

Micronemacheilus pulcherimus	China	Guangxi	Pearl	A8690 A8691	PP280043 PP280044	PP315878 PP315879	PP280229 PP280230	PP280508 PP280509	PP259968 PP259969	PP259700 -
Oreonectes guananensis	China	Guangxi	Pearl	GenBank	ON116507	OP473623	OP473878	OP473665	OP473750	OP473830
Oreonectes luochengensis	China	Guangxi	Pearl	GenBank	ON116495	-	OP473882	OP473670	OP473749	OP473836
Oreonectes platycephalus	China	Hong Kong	Tai Tam	A1674 A1675 A1676 GenBank	PP279902 PP279903 PP279904 ON116528	PP315737 PP315738 PP315739 OP473652	PP280115 PP280116 PP280117 OP473904	PP280323 PP280324 PP280325 OP473696	PP259777 PP259778 PP259779 OP473745	- - - OP473862
Oreonectes* cf. *platycephalus 1	China	Guangxi	Pearl	A9065	PP280053	PP315888	PP280239	PP280518	PP259977	PP259707
Oreonectes* cf. *platycephalus 2	China	Guangxi	Pearl	A8697	PP280045	PP315880	PP280231	PP280510	PP259970	PP259701
Oreonectes* cf. *platycephalus 3	Vietnam	Lang Son	Pearl	A10603	PP279881	-	-	PP280292	-	-
Oreonectes polystigmus	China	Guangxi	Pearl	GenBank	ON116514	OP473614	OP473871	OP473657	OP473746	OP473856
***Oreonectes* sp.**	China	Guangxi	Pearl	A8963 A8964	PP280047 PP280048	PP315882 PP315883	PP280233 PP280234	PP280512 PP280513	PP259972 -	PP259702 PP259703
Paranemachilus genilepis	China	Guangxi	Pearl	GenBank	ON116497	OP473630	OP473885	OP473673	OP473752	OP473839
Paranemachilus pingguoensis	China	Guangxi	Pearl	GenBank	ON116500	OP473634	OP473888	OP473676	OP473755	OP473843
Paranemachilus zhengbaoshani	China	Guangxi	Pearl	A9153	PP280054	PP315889	PP280240	PP280519	PP259978	PP259708
Sundoreonectes sabanus	Malaysia	Sabah	Baram	A1844 A1845	PP279914 PP279915	PP315748 PP315749	PP280126 PP280127	PP280334 PP280335	PP259789 PP259790	PP259651 PP259652

Traccatichthys pulcher	China	Guangxi	Pearl	A1804	PP279910	PP315744	PP280122	PP280330	PP259785	-
				A1805	PP279911	PP315745	PP280123	PP280331	PP259786	-
				A8681	PP280042	PP315877	PP280228	PP280507	PP259967	PP259699
Traccatichthys taeniatus	Vietnam	Nghe An	Lam	A3175	PP279960	PP315796	PP280167	PP280387	PP259840	PP259666
				A3176	PP279961	PP315797	PP280168	PP280388	PP259841	-
	Laos	Houaphan	Mekong	CMK 25931	PP279871	PP315710	PP280088	PP280249	PP259738	-
Traccatichthys* cf. *taeniatus	Vietnam	Quang Nam	Cau Do	A9575	PP280060	-	-	-	-	-
Traccatichthys zispi	China	Hainan	-	GenBank	ON116518	OP473648	OP473898	OP473691	OP473780	OP473861
Troglonectes barbatus	China	Guizhou	Pearl	GenBank	ON116501	OP473635	OP473889	OP473678	OP473756	-
Troglonectes daqikongensis	China	Guizhou	Pearl	GenBank	ON116526	OP473641	-	OP473683	OP473773	OP473849
Troglonectes dongganensis	China	Guangxi	Pearl	GenBank	ON116503	OP473617	OP473875	OP473661	OP473757	OP473847
Troglonectes donglanensis	China	Guangxi	Pearl	GenBank	ON116505	OP473621	OP473877	OP473663	OP473762	OP473826
Troglonectes duanensis	China	Guangxi	Pearl	GenBank	ON116509	OP473622	OP473880	OP473667	OP473764	OP473831
Troglonectes elongatus	China	Guangxi	Pearl	GenBank	ON116502	OP473616	OP473874	OP473660	OP473758	OP473848
Troglonectes furcocaudalis	China	Guangxi	Pearl	GenBank	ON116512	OP473628	OP473883	OP473671	OP473767	OP473837
Troglonectes jiarongensis	China	Guizhou	Pearl	GenBank	ON116527	OP473643	OP473894	OP473685	OP473769	OP473846
Troglonectes lihuensis	China	Guangxi	Pearl	GenBank	ON148332	OP473618	OP473892	OP473688	-	OP473852

Troglonectes macrolepis	China	Guangxi	Pearl	GenBank	ON116498	OP473632	OP473886	OP473674	OP473753	OP473841
Troglonectes microphthalmus	China	Guangxi	Pearl	A8988 A8989 GenBank	PP280049 PP280050 ON116494	PP315884 PP315885 OP473631	PP280235 PP280236 OP473872	PP280514 PP280515 OP473659	PP259973 PP259974 OP473748	PP259704 PP259705 OP473840
Troglonectes retrodorsalis	China	Guangxi	Pearl	GenBank	ON116511	OP473627	OP473873	OP473669	OP473766	OP473835
Troglonectes shuilongensis	China	Guizhou	Pearl	GenBank	ON116522	OP473636	OP473891	OP473679	OP473768	OP473834
Troglonectes translucens	China	Guangxi	Pearl	GenBank	ON116510	OP473626	OP473881	OP473668	OP473765	OP473832
Yunnanilus pleurotaenia	China	Yunnan	Yangtze	A2967 A2968 A2969	PP279954 PP279955 PP279956	PP315791 PP315792 PP315793	PP280163 PP280164 PP280165	PP280381 PP280382 PP280383	PP259836 PP259837 PP259838	PP259664 PP259665 -
NORTHERN CLADE										
Barbatula altayensis	Mongolia	Khovd	Bulgan Gol	CMK19584_1 CMK19584_2	PP279850 PP279851	PP315685 PP315686	PP280069 PP280070	PP280259 PP280260	PP259718 PP259719	PP259627 -
Barbatula barbatula	France Russia Germany Czechia	Haute-Garonne Unknown Nordrhein-Westfalen Liberecky	Garonne unknown Rhine Elbe	CMK19464_1CMK19464_2 A4013 A4015 A2046 A2047 A2587	PP279842 PP279843 PP279979 PP279980 PP279922 PP279923 PP279923 PP279941	PP315677 PP315678 PP315816 PP315817 PP315756 PP315757 PP315777 PP315778	- - PP280179 PP280180 PP280133 PP280134 PP280150 PP280151	PP280251 PP280252 PP280409 PP280410 PP280344 PP280345 PP280367 PP280368	- PP259711 PP259858 - PP259798 PP259799 PP259822 PP259823	- PP259624 - PP259674 PP259655 - - -

	Czechia	Stredocesky	Elbe	A2588	KP738604	KP738564	KP738524	PP280499	PP259955	PP259697
				A8393	KP738605	KP738565	KP738525	OL191359	PP259956	-
	Poland	Dolnośląskie	Oder	A8394	PP279952	PP315789	PP280161	PP280379	PP259834	-
				A2957	PP279953	PP315790	PP280162	PP280380	PP259835	-
				A2958						
Barbatula compressirostris	Mongolia	Khovd	Khovd Tsendkhar	CMK19564_1	PP279848	PP315683	PP280067	PP280257	PP259716	PP259626
					PP279849	PP315684	PP280068	PP280258	PP259717	-
	Mongolia	Khovd	Khovd	CMK19564_2	PP279852	PP315687	PP280071	PP280261	PP259720	PP259628
					PP279853	PP315688	PP280072	PP280262	PP259721	-
				CMK19590_1CMK19590_2						
Barbatula dgebuadzei	Mongolia	Bayankhongor	Baydrag	CMK19594_1	PP279854	PP315689	PP280073	PP280263	PP259722	PP259629
					PP279855	PP315690	PP280074	PP280264	PP259723	-
				CMK19594_2						
Triplophysa labiata	Kazachstan	Almaty	Lake Balkash	A5381	PP280005	PP315842	-	PP280448	PP259896	-
				A5384	PP280008	PP315845	PP280197	PP280451	PP259899	-
				A5385	PP280009	PP315846	PP280198	PP280452	PP259900	-
Barbatula oreas	Japan	Hokkaido	Shinkawa	A11223	PP279887	PP315722	PP280097	PP280300	PP259754	PP259638
				A11224	PP279888	PP315723	PP280098	PP280301	PP259755	-
***Barbatula* sp. Korea**	Korea	Gangwon	Cheon Jin Cheon	A1888	PP279918	PP315752	-	PP280340	-	-
***Barbatula* sp. Tuul**	Mongolia	Ulaanbaatar	Yenisey	A4246	PP279981	-	-	PP280412	PP259861	PP259676
				A4247	PP279982	PP315818	PP280181	PP280413	-	-
				A4248	PP279983	PP315819	PP280182	PP280414	PP259862	-
				A4250	PP279985	PP315821	PP280184	PP280416	PP259863	-
Barbatula toni	Russia	Primorsky	Amur	A3171	PP279959	-	-	PP280386	-	-

Barbatula* cf. *toni	Mongolia Mongolia	Khövgöl Ulaanbaatar	Yenisey Yenisey	CMK19540_1 CMK19540_2A4249	PP279844 PP279845 PP279984	PP315679 PP315680 PP315820	PP280063 PP280064 PP280183	PP280253 PP280254 PP280415	PP259712 PP259713 -	- - PP259677
Claea dabryi	China	Sichuan	Yangtze	GenBank	MG238214	MG237922	MG238312	-	MG238015	-
Triplophysa baotianensis	China	Guizhou	Pearl	GenBank	MT992550	OP473612	OP473868	OP473655	-	OP473864
Triplophysa bleekeri	China	no detail	Yangtze	GenBank	MG238298 KX373847	MG238003 MG725561	MG238415 MG698830	- MG698529	- MG697779	- -
Triplophysa brevicauda	China	no detail	Yangtze	GenBank	MG238300	MG238005	MG238417	-	MG238107	-
Triplophysa dalaica	China	Gansu	no details	GenBank	MG697586	-	MG698831	MG698530	MG697806	-
Triplophysa dorsalis	Kazachstan	Almaty	Lake Balkash	A5377 A5378 A5380 A5383	PP280001 PP280002 PP280004 PP280007	PP315838 PP315839 PP315841 PP315844	PP280191 PP280192 PP280194 PP280196	PP280444 PP280445 PP280447 PP280450	PP259893 PP259894 PP259895 PP259898	PP259684 PP259685 - -
Triplophysa grahami	China	Yunnan	Yangtze	A1663 A2933	MK608125 PP279948	OL191414 PP315785	MT536722 -	OL191277 PP280375	PP259776 PP259830	PP259648 -
Triplophysa gundriseri	Mongolia	Khövgöl	Tes Gol	CMK19543_1 CMK19543_2	PP279846 PP279847	PP315681 PP315682	PP280065 PP280066	PP280255 PP280256	PP259714 PP259715	PP259625 -
Triplophysa huapingensis	China	Guangxi	Pearl	GenBank	MG697589	-	MG698834	MG698537	MG697870	-

Triplophysa leptosoma	China	no detail	Yangtze	GenBank	KX373839	-	MG698825	MG698524	MG697601	-
Triplophysa luochengensis	China	Guangxi	Pearl	A8990 A8991	PP280051 PP280052	PP315886 PP315887	PP280237 PP280238	PP280516 PP280517	PP259975 PP259976	PP259706 -
Triplophysa nandanensis	China	Guangxi	Pearl	GenBank	MG697588	-	MG698833	MG698536	MG697869	-
Triplophysa nanpanjiangensis	China	Yunnan	Pearl	GenBank	MG238302	MG238007	MG238419	-	MG238109	-
Triplophysa nasobarbatula	China	Guizhou	Pearl	GenBank	ON116529	OP473653	OP473869	OP473697	OP473781	OP473865
Triplophysa obscura	China	no detail	Yangtze	GenBank	MG238304	MG238009	MG238421	-	MG238111	-
Triplophysa orientalis	China	Qinghai	Yangtze	GenBank	KX373846	-	MG698829	MG698528	MG697755	-
Triplophysa pseudoscleroptera	China	Qinghai	Yangtze	GenBank	MG697585	-	MG698828	MG698527	MG697684	-
Triplophysa rosa	China	Wulong	Yangtze	GenBank	MG697587	MG725565	MG698832	MG698535	MG697868	-
Triplophysa scleroptera	China	No details	Yangtze	GenBank	MG238307 KX373833	MG238012 MG725554	MG238424 MG698838	MG698534	MG238113 MG697908	- -
Triplophysa siluroides	China	no details	no details	1797	MT536720	EF063156	MT536723	OL191278	PP259784	PP259650
Triplophysa stenura	China	Yunnan	Yangtze	2935 2938 2939	PP279949 PP279950 PP279951	PP315786 PP315787 PP315788	PP280158 PP280159 PP280160	PP280376 PP280377 PP280378	PP259831 PP259832 PP259833	- PP259662 PP259663

				GenBank	MG697583	MG725550	MG698824	MG698523	MG697592	-
Triplophysa stolickai	China	no detail	no details	GenBank	MG697582	MG725535	MG698822	MG698521	MG697590	-
Triplophysa strauchi	Kazachstan Kyrgyzstan	Almaty Naryn	Lake Balkash Syr Darya	5367 5379 5382 11496 11497	PP280000 PP280003 PP280006 MT536721 PP279889	- PP315840 PP315843 OL191500 PP315725	- PP280193 PP280195 MT536724 PP280100	- PP280446 PP280449 OL191382 PP280303	- - PP259897 PP259757 PP259758	- PP259686 - PP259639 -
Triplophysa tenuis	China	no detail	no details	GenBank	MG697584	MG725556	MG698827	MG698526	MG697626	-
Triplophysa wuweiensis	China	Gansu	no details	GenBank	KX373838	-	MG698823	MG698522	MG697591	-
INDOCHINESE CLADE										
Homatula anguillioides	China	Yunnan	Mekong	GenBank	HM010583	HM010669	MG238315	-	MG238018	-
Homatula change	China	Yunnan	Mekong	GenBank	-	-	MG238318	-	MG238021	-
Homatula cryptoclathrata	China	Yunnan	Salween	GenBank	HM010569	HM010663	MG238332	-	-	-
Homatula disparizona	China	Yunnan	Red	GenBank	MG238218	MG237926	MG238321	-	MG238023	-
Homatula laxiclathra	China	Shanxi	Yellow	GenBank	MG238219	MG237927	MG238322	-	MG238024	-
Homatula longidorsalis	China	Yunnan	Pearl	GenBank	HM010522	HM010618	MG238324	-	MG238026	-

Homatula potanini	China	Sichuan	Yangtze	A1788 A1789	PP279908 PP279909	PP315742 PP315743	PP280120 PP280121	PP280328 PP280329	PP259782 PP259783	PP259649 -
Homatula pycnolepis	China	Yunnan	Mekong	A2973	PP279957	PP315794	PP280166	PP280384	PP259839	-
Homatula variegata	China	Sichuan	Yangtze	A1459 A1460	PP279900 PP279901	PP315735 PP315736	PP280112 PP280113	PP280319 PP280320	PP259773 PP259774	PP259646 -
Homatula wuliangensis	China	Yunnan	Mekong	GenBank	HM010517	HM010609	MG238336	-	MG238036	-
'Nemacheilus' arenicolus	Laos	Bolikhamsay	Mekong	CMK21208_2 CMK21208_3	MW512964 MW512965	MW513090 MW513091	MW513213 MW513214	PP280265 PP280266	PP259724 PP259725	- PP259630
'Nemacheilus' argyrogaster	Laos	Sekong	Mekong	CMK21521_1 CMK21521_2	MW512988 MW512989	MW513111 MW513112	MW513237 MW513238	PP280267 PP280268	PP259726 PP259727	PP259631 -
'Nemacheilus' banar	Vietnam	Kontum	Mekong	A3307 A3308	PP279967 MW512968	PP315803 MW513094	PP280172 MW513217	PP280396 PP280397	PP259849 PP259850	PP259672 -
'Nemacheilus' cleopatra	Vietnam	Gia Lai	Song Ba	A3256 A3257	MW512982 MW512983	MW513106 MW513107	MW513231 MW513232	PP280392 PP280393	PP259845 PP259846	PP259669 -
Rhyacoschistura suber	Laos Laos	Xiengkhuang Xaysomboon	Mekong Mekong	CMK22643 CMK22484	PP279857 PP279856	PP315692 PP315691	- PP280079	PP280270 PP280269	PP259729 PP259728	PP259632 -
Schistura amplizona	China	Yunnan	Mekong	GenBank	MG238243	MG237949	MG238357	-	MG238056	-
Schistura bolavensis	Laos	Champasak	Mekong	A4618 A4620	KP738575 KP738576	KP738535 KP738536	KP738495 KP738496	OL191315 PP280421	PP259869 PP259870	PP259681 -

Schistura bucculenta	China	Yunnan	Mekong	GenBank	JN837654	JN837666	-	-	-	-
Schistura callichroma	China	Yunnan	Red	GenBank	MG238244	MG237950	MG238359	-	MG238057	-
Schistura caudofurca	China	Yunnan	Red	GenBank	MG238245	MG237951	MG238360	-	MG238059	-
Schistura* cf. *amplizona	Thailand	Loei	Mekong	A2375	PP279932	PP315766	PP280144	PP280355	PP259808	PP259658
Schistura* cf. *palma	Thailand	Loei	Mekong	2376	PP279933	PP315767	-	PP280356	PP259809	PP259659
Schistura* cf. *schultzei	Thailand	Loei	Mekong	2522 2523	PP279934 PP279935	PP315768 PP315769	PP280145 PP280146	PP280359 PP280360	PP259813 PP259814	PP259660 -
Schistura cryptofasciata	China	Yunnan	Salween	GenBank	MG238250	MG237956	MG238366	-	MG238063	-
Schistura desmotes	Thailand	Chiang Mai	Chao Phraya	A1180 A1181 A1182	PP279892 PP279893 PP279894	PP315728 PP315729 PP315730	- - -	PP280306 PP280307 PP280308	PP259761 PP259762 PP259763	PP259640 - -
Schistura dubia	Thailand	Phrae	Chao Phraya	GenBank	MK301364	-	-	-	-	-
Schistura fasciolata	China	Guangxi	Pearl	A5300 A5301 A5302	KP738579 KP738580 KP738581	KP738539 KP738540 KP738541	KP738499 KP738500 KP738501	PP280441 PP280442 OL191323	PP259888 PP259889 PP259890	PP259683 - -
Schistura fusinotata	Laos	Xekong	Mekong	A5065	PP279991	PP315830	PP280188	PP280430	PP259880	-
Schistura implicata	Vietnam	Lam Dong	Mekong	GenBank	MG238289	MG237995	MG238406	-	-	-
Schistura incerta	China	No details	No details	GenBank	MK361215	KP695623	KP695078	-	KP695739	KP694654
Schistura* sp. *Lam	Vietnam	Nghe An	Lam	A3198 A3199	PP279962 PP279963	PP315798 PP315799	PP280169 PP280170	PP280389 PP280390	PP259842 PP259843	PP259667 -

Schistura irregularis	Laos	Houaphan	Mekong	CMK25919_1 CMK25919_2	PP279866 PP279867	PP315701 PP315702	PP280084 PP280085	PP280279 PP280280	- -	PP259635 -
Schistura kaysonei	Laos	Bolikhamsay	Mekong	GenBank	NC_031580	-	-	-	-	-
Schistura klydonion	Laos	Champasak	Mekong	CMK23320_1 CMK23320_2	PP279858 PP279859	PP315693 PP315694	PP280080 PP280081	PP280271 PP280272	PP259980 PP259981	PP259709 -
Schistura kongphengi	Vietnam	Thua Thien Hue	Mekong	A2722 A3321	PP279945 PP279969	PP315782 PP315805	PP280155 PP280173	PP280372 PP280399	PP259827 PP259851	- -
Schistura laterimaculata	Thailand	Petchabun	Mekong	A6848 A6849	PP280023 PP280024	PP315856 PP315857	PP280208 PP280209	PP280465 PP280466	PP259922 PP259923	PP259689 -
Schistura latidens	China	Yunnan	Mekong	GenBank	MG238266	MG237973	MG238383	-	MG238081	-
Schistura latifasciata	China	Yunnan	Mekong	GenBank	MG238268	MG237975	MG238385	-	MG238083	-
Schistura macrocephala	China	Yunnan	Mekong	GenBank	MG238274	MG237981	MG238391	-	MG238088	-
Schistura macrotaenia	China	Yunnan	Mekong	GenBank	JN837655	JN837667	-	-	-	-
Schistura magnifluvis	China	Yunnan	Mekong	GenBank	JN837654	MG237967	MG238355	-	MG238075	-
Schistura moeiensis	Thailand	Tak	Salween	A4965 A4966 A11033	PP279988 PP279989 PP279883	PP315826 PP315827 PP315718	PP280185 PP280186 PP280094	PP280426 PP280427 PP280296	PP259876 PP259877 PP259752	- - -
Schistura nicholsi	China	Yunnan	Mekong	GenBank	DQ105202	-	-	-	-	-

Schistura notasileum	China	Yunnan	Mekong	GenBank	OQ945050	OQ973300	OQ973298	-	OQ973302	-
Schistura porthos	China	Yunnan	Mekong	GenBank	MG238282	MG237988	MG238399	-	-	-
Schistura reidi	Thailand	Mae Hong Son	Salween	A781 A817	PP280032 PP280036	PP315865 PP315871	PP280217 PP280220	PP280488 PP280494	PP259950 -	- -
Schistura rikiki	Laos	Xekong	Mekong	A5066 A5067	PP279992 PP279993	PP315831 PP315832	PP280189 PP280190	PP280431 PP280432	PP259881 -	PP259682 -
Schistura sertata	Laos	Luang Prabang	Mekong	A2531 A2531	PP279936 PP279937	PP315770 PP315771	PP280147 PP280148	PP280361 PP280362	PP259815 PP259816	- -
Schistura sexcauda	Thailand	Chiang Mai	Chao Phraya	A755	PP280029	PP315862	PP280214	PP280485	PP259947	-
Schistura similis	Thailand	Tak	Salween	A5004	PP279990	PP315828	PP280187	PP280428	PP259878	-
Schistura sokolovi	Vietnam	Gia Lei	Song Ba	A3384	PP279970	PP315806	PP280174	PP280400	PP259852	PP259673
Schistura susannae	Vietnam	Da Nang	Mong Mo	GenBank	MG238288	MG237994	MG238405	-	-	-
Schistura thanho	Vietnam	Bien Dinh	Vinh Thanh	A3310	PP279968	PP315804	-	PP280398	-	-
Schistura waltoni	Thailand	Chiang Mai	Chao Phraya	A731 A732	PP280027 PP280028	PP315860 PP315861	PP280212 PP280213	PP280477 PP280478	PP259934 PP259935	- -
Schistura xhatensis	Laos	Houaphan	Mekong	CMK25920_1 CMK25920_2	PP279868 PP279869	PP315703 PP315704	PP280086 PP280087	PP280281 PP280282	PP259736 PP259737	PP259636 -
Schistura yersini	Vietnam	Lam Dong	Da Dung	A3206	PP279964	PP315800	PP280171	PP280391	PP259844	PP259668
Sectoria atriceps	Thailand	Nan	Chao Phraya	A845 A846 A847	PP280037 PP280038 PP280039	PP315872 PP315873 PP315874	PP280221 PP280222 PP280223	PP280500 PP280501 PP280502	PP259957 PP259960 PP259961	- - -

				A848 A849	PP280040 PP280041	PP315875 PP315876	PP280224 PP280225	PP280503 PP280504	PP259962 PP259963	- PP259698
Sectoria heterognathos	Laos	Louang Namtha	Mekong	CMK25980	PP279872	PP315705	PP280089	PP280283	PP259740	-
Speonectes tiomanensis	Malaysia	Pahang	No detail	A1848 A1849	PP279916 PP279917	PP315750 PP315751	PP280128 PP280129	PP280336 PP280337	PP259791 PP259792	- -
Tuberoschistura baenzingeri	Thailand	Surat Thani	Tapi	A2340 A4485	- -	PP315765 PP315822	PP280143 -	PP280354 PP280418	PP259807 PP259866	PP259657 -
Tuberoschistura cambodgiensis	Cambodia	Phnom Penh	Mekong	A7949 A7950	- -	PP315866 PP315867	PP280218 PP280219	PP280489 PP280490	PP259951 PP259952	PP259696 -
SUNDAIC CLADE										
Nemacheilus binotatus	Thailand	Chiang Mai	Chao Phraya	A6926 A6927	KP738586 KP738587	KP738546 KP738547	KP738506 PP280210	OL191346 PP280469	PP259926 PP259927	PP259690 -
Nemacheilus cacao	Laos	Bolikhamsay	Mekong	ZRC 62554 ZRC 62553	ON720269 ON720270	ON720271 ON720272	PP280244 PP280245	PP280527 PP280528	PP259983 -	- -
Nemacheilus* cf. *tuberigum	Indonesia	Aceh	Alas	A4536 A4537	PP279986 PP279987	PP315823 PP315824	- -	PP280419 PP280420	PP259867 PP259868	PP259680 -
Nemacheilus masyae	Thailand Cambodia	Surat Thani Siem Reap	Tapi Mekong	A1421 A1422 A5450	MW512997 MW512998 PP280010	MW513120 MW513121 PP315847	PP280109 PP280110 PP280199	PP280316 PP280317 PP280453	PP259771 PP259772 PP259901	PP259644 - -
Nemacheilus ornatus	Thailand	Surat Thani	Tapi	A1402 A1403	MW513023 MW513024	MW513146 MW513146	PP280107 PP280108	PP280314 PP280315	PP259769 PP259770	PP259643 -

Nemacheilus pallidus	Thailand	Nan	Chao Phraya	A1394	MW513029	MW513151	PP280106	PP280313	PP259768	-
Nemacheilus platyceps	Thailand	Chanthaburi	Mekong	A856 A857	MW513045 MW513046	MW513170 MW513171	PP280226 PP280227	PP280505 PP280506	PP259965 PP259966	- -
Nemacheilus saravacensis	Malaysia	Sarawak	Sabang	A1632	MW513056	MW513181	PP280114	PP280321	PP259775	-
Nemacheilus selangoricus	Thailand	Nakhon Si Thammarat	Pak Paying	A1437	MW513062	MW513186	PP280111	PP280318	-	PP259645
Nemacheilus spiniferus	Malaysia	Sarawak	Engkaban	A1640	MW513079	MW513203	-	PP280322	-	PP259647
BURMESE CLADE										
Aborichthys kempi	Myanmar	Kachin	Irrawaddy	CMK25538_1 CMK25538_2	PP280061 PP280062	PP315697 PP315698	- -	PP280275 PP280276	PP259732 PP259733	PP259633 -
***Aborichthys* sp.**	India	West Bengal	Brahma-putra	A3972 A3973	PP279977 PP279978	PP315814 PP315815	PP280177 PP280178	PP280407 PP280408	PP259857 -	- -
Acanthocobitis* cf. *pavonacea	Ornamental fish trade			A1863 A1864	MK608119 MK608120	EF056379 MK608146	MK608242 MK608243	PP280338 PP280339	PP259794 PP259795	- -
Paracanthocobitis epimekes	Thailand Myanmar	Phang Nga Tanintharyi	Takua Pa	A2460 CMK 24940	MK608038 MK608104	MK608151	MK608248 MK608307	PP280357 PP280247	PP259811 PP259730	- -

			Tenasserim			MK608213				
Paracanthocobitis linypha	Myanmar	no details		A2562 A2563	MK608044 MK608045	MK608157 MK608158	MK608254 MK608255	PP280365 PP280366	PP259821 -	- -
Paracanthocobitis mackenziei	Ornamental Nepal	fish trade Koshi	 Ganges	A82 A83 A3437	EF508598 MK608121 MK608113	EF056383 MK608127 MK608162	MK608221 MK608222 MK608259	PP280495 PP280496 PP280401	- - PP259853	- - -
Paracanthocobitis mandalayensis	Thailand	Tak	Salween	A11558	PP279890	PP315726	-	PP280304	PP259759	-
Paracanthocobitis phuketensis	Myanmar Thailand Thailand Thailand Thailand	Tanintharyi Phatthalung Trang Phang Nga Phang Nga	Tenasserim Phaniat Palian Tam Nang Takua Pa	CMK 24909 A5190 A5175 A9713 A2466	MK608107 MK608075 MK608071 MK608099 MK608042	MK608216 MK608186 MK608182 MK608208 MK608155	MK608310 MK608281 MK608277 MK608302 MK608252	PP280246 PP280434 PP280433 PP280526 PP280358	- PP259882 - - PP259812	- - - - -
Paracanthocobitis pictilis	Ornamental	fish trade		A6940 A6941 A10938	KP738589 KP738590 PP279882	KP738549 KP738550 PP315715	KP738509 KP738510 -	OL191347 PP280471 PP280293	PP259929 - PP259749	PP259692 - -
***Paracanthocobitis* sp. Irrawaddy**	Myanmar Myanmar	Magway Ayeyerwady	Irrawaddy Irrawaddy	A5774 A6621 A6573	MK608078 MK608089 MK608086	MK608189	MK608284 MK608293 MK608291	PP280456 PP280459 PP280458	PP259905 - PP259912	- - -

						MK608198 MK608196				
***Paracanthocobitis* sp. Rakhine**	Myanmar	Rakhine	no details	A5331 A5332	KP738582 KP738583	KP738542 KP738543	KP738502 KP738503	OL191324 PP280443	PP259891 PP259892	- -
***Paracanthocobitis* sp. Sittaung**	Myanmar	Mon	Sittaung	A4102	MK608051	MK608164	MK608261	PP280411	-	-
Paracanthocobitis zonalternans	Thailand	Tak	Salween	A4942	MK608065	MK608176	MK608271	PP280425	-	-
Schistura* cf. *kohchangensis	Thailand	Tak	Salween	A11046	PP279884	PP315719	PP280095	PP280297	PP259753	-
Schistura kohchangensis	Thailand	Chanthaburi	Mekong	A1822 A1823	PP279912 PP279913	PP315746 PP315747	PP280124 PP280125	PP280332 PP280333	PP259787 PP259788	- -
Schistura savona	Ornamental fish trade			A7530 A7532	KP738598 KP738599	KP738558 KP738559	KP738518 KP738519	PP280482 OL191354	PP259939 PP259940	PP259695 -
SOUTHERN CLADE										
Afronemacheilus abyssinicus	Ethiopia	Amhara	Nile	A11680	PP279891	PP315727	PP280101	PP280305	PP259760	-
Mesonoemacheilus guentheri	India	Ornamental fish trade		A2630 A2631 A6935	PP279943 PP279944	PP315780 PP315781	PP280153 PP280154	PP280370 PP280371 PP280470	PP259825 PP259826 PP259928	- - PP259691
Mesonoemacheilus herrei	India	Tamil Nadu	Periyar	A5526 A5527	PP280011 PP280012	PP315848 PP315849	PP280200 PP280201	PP280454 PP280455	PP259902 PP259903	- -
Mesonoemacheilus pambarensis	India	Tamil Nadu	Pambar	GenBank	MF680101	-	-	-	-	-

Mesonoemacheilus petrubanarescui	India	Karnataka	Saklshpur	A9197	PP280055	PP315890	PP280241	PP280520	PP259979	-
Mesonoemacheilus tambaraparniensis	India	Tamil Nadu	Tamiraparani	GenBank	MF680096	-	-	-	-	-
Mesonoemacheilus triangularis	India	Ornamental fish trade		A944 A945	PP280058 PP280059	PP315891 PP315892	PP280242 PP280243	PP280521 PP280522	PP259984 PP259985	- -
Mustura bella	Laos	Louang Namtha	Mekong	CMK 26052	OL191242	OL191491	OL345558	OL191373	PP259743	-
Mustura celata	Myanmar	Kachin	Irrawaddy	CMK25620_1 CMK25620_2	PP279863 PP279864	PP315699 PP315700	PP280082 PP280083	PP280277 PP280278	PP259734 PP259735	PP259634 -
Mustura geisleri	Thailand	Chiang Mai	Chao Phraya	A1238 A1239	OL191158 OL191159	OL191407 OL191408	OL345477 OL345478	OL191270 OL191271	PP259764 PP259765	- -
Mustura isostigma	Laos	Khammouane	Mekong	A1307	PP279899	-	-	-	-	-
Mustura maepaiensis	Thailand	Mae Hong Son	Salween	A799 A804 A805	PP280033 PP280034 PP280035	PP315868 PP315869 PP315870	- - -	PP280491 PP280492 PP280493	- - -	- - -
Mustura shanensis	Myanmar	Shan	Salween	A6649 A6773 A6774	OL191213 OL191220 OL191221	OL191462 OL191469 OL191470	OL345529 OL345536 OL345537	OL191333 OL191340 OL191341	PP259913 - PP259920	- PP259688 -
***Mustura* sp.**	Myanmar	Magway	Irrawaddy	A6712 A6713	PP280019 PP280020	PP315852 PP315853	PP280204 PP280205	PP280461 PP280462	PP259917 -	- -
***Mustura* sp. Salween**	Thailand	Tak	Salween	A1776	PP279907	-	-	-	-	-

Nemachilichthys ruppelli	India	Ornamental fish trade		A4341 A4345	KP738573 KP738574	KP738533 KP738534	KP738493 KP738494	OL191311 PP280417	PP259864 PP259865	PP259678 PP259679
Neonoemacheilus labeosus	Thailand	Tak	Salween	A1774 A1775	PP279905 PP279906	PP315740 PP315741	PP280118 PP280119	PP280326 PP280327	PP259780 PP259781	- -
Neonoemacheilus peguensis	Myanmar	Bago	Sittaung	A877	PP280046	PP315881	PP280232	PP280511	PP259971	-
***Neonoemacheilus* sp. Irrawaddy**	Myanmar	Magway	Irrawaddy	A6287	PP280017	PP315850	PP280202	PP280457	PP259909	-
***Neonoemacheilus* sp.**	Myanmar	Magway	Irrawaddy	A6664 A6734 A6735	PP280018 PP280021 PP280022	PP315851 PP315854 PP315855	PP280203 PP280206 PP280207	PP280460 PP280463 PP280464	PP259914 - -	- - -
Oxynoemacheilus angorae	No details			GenBank	NC_031548	-	-	-	-	-
Oxynoemacheilus brandtii	Armenia	Lori	Kura	A3901 A3902	PP279975 PP279976	PP315812 PP315813	- -	PP280405 PP280406	- -	- -
Oxynoemacheilus bureschi	Bulgaria	Blagoevgrad	Struma	A12147 A12148	PP279895 PP279896	PP315731 PP315732	PP280102 PP280103	PP280309 PP280310	PP259991 PP259992	PP259641 -
Oxynoemacheilus cilicic	Turkey	Adana	Seyhan	A2758	PP279947	PP315784	PP280157	PP280374	PP259828	-
Oxynoemacheilus chomanicus	Iran	Kurdistan	Tigris	GenBank	KT715806	-	-	-	-	-
Oxynoemacheilus euphraticus	Turkey	Mus	Euphrat	A1003	PP279876	PP315708	PP280090	PP280286	-	-
Oxynoemacheilus frenatus	Turkey	Diyarbakir	Tigris	A2102 A2103	PP279926 PP279927	PP315759 PP315760	PP280137 PP280138	PP280348 PP280349	- -	- -
Oxynoemacheilus galilaeus	Syria	Dara	Jordan	A3890 A3891	PP279973 PP279974	PP315810 PP315811	- PP280176	- -	- -	- -
Oxynoemacheilus gyndes	Iraq	Sulaimaniyah	Tigris	GenBank	MH842968	MH843091	-	-	-	-

Oxynoemacheilus hanae	Iraq	Sulaimaniyah	Tigris	GenBank	MH842969	MH843092	-	-	-	-
***Oxynoemacheilus* veyselorum**	Turkey	Erzurum	Arax	A1045	PP279877	PP315709	-	PP280287	-	-
Oxynoemacheilus insignis	Israel	West bank	Jordan	A1961 A1962	PP279920 PP279921	PP315754 PP315755	PP280131 PP280132	PP280342 PP280343	PP259796 PP259797	PP259654 -
***Oxynoemacheilus kaynaki* 1**	Turkey	Elazig	Euphrat	A1000	PP279874	PP315706	-	PP280284	-	-
***Oxynoemacheilus kaynaki* 2**	Turkey	Elazig	Euphrat	A1002	PP279875	PP315707	-	PP280285	-	-
Oxynoemacheilus kurdistanicus	Iran	Kurdistan	Tigris	GenBank	KU180210	-	-	-	-	-
Oxynoemacheilus merga	Russia	Dagestan	Rubas	A1109 A1110	PP279885 PP279886	PP315720 PP315721	PP280096 -	PP280298 PP280299	- -	PP259637 -
Oxynoemacheilus persa	Iran	Fars	Kor	A695 A697	PP280025 PP280026	PP315858 PP315859	PP280211 -	PP280474 PP280476	PP259933 -	- -
Oxynoemacheilus phasicus	Georgia	Imereti	Rioni	A2057	PP279924	-	PP280135	PP280346	PP259800	-
Oxynoemacheilus pindus	Albania	Gjirokaster	Vjosa	A12149 A12150	PP279897 PP279898	PP315733 PP315734	PP280104 PP280105	PP280311 PP280312	PP259993 PP259994	PP259642 -
***Oxynoemacheilus* sp. Turkey**	Turkey	No details	No details	GenBank	EU015983	-	-	-	-	-
Oxynoemacheilus tongiorgii	Iran	Fars	Kor	A2757	PP279946	PP315783	PP280156	PP280373	-	-
Oxynoemacheilus zagrosensis	Iran	Kurdistan	Tigris	GenBank	KU180203	-	-	-	-	-
Oxynoemacheilus zarzianus	Iraq	Al-Sulaimaniyah	Tigris	GenBank	KY849795	-	-	-	-	-

Paracobitis atrakensis	Iran	Khorasane - Shomali	Atrak	GenBank	MG229862	-	-	-	-	-
Paracobitis hircanica	Iran	Golestan	Gorgan Roud	A2186 A2187 A2188	PP279928 PP279929 PP279930	PP315761 PP315762 PP315763	PP280139 PP280140 PP280141	PP280350 PP280351 PP280352	PP259802 PP259803 PP259804	PP259656 - -
Paracobitis malapterura	Iran	Qom	Emamzadeh Abdollah	GenBank	MG229879	-	-	-	-	-
Paracobitis molavii	Iran	West Azerbaijan	Tigris	GenBank	MG229860	-	-	-	-	-
Paracobitis persa	Iran	Fars	Kor	GenBank	MG229866	-	-	-	-	-
Paracobitis rhadinaea	Iran	Sistan and Baluchistan	Sistan	GenBank	MG229870	-	-	-	-	-
Paraschistura cristata	Iran	Khorazan Razavi	Hari	A5262 A5263 A5264 A5265 A5266	PP279995 PP279996 PP279997 PP279998 PP279999	PP315833 PP315834 PP315835 PP315836 PP315837	- - - - -	PP280436 PP280437 PP280438 PP280439 PP280440	PP259883 PP259884 PP259885 PP259886 PP259887	- - - - -
Paraschistura montana	India	No details	Ganges	GenBank	FJ711438	-	-	-	-	-
Petruichthys brevis	Myanmar	Shan	Salween	A4184 A4185 A6503 A6739	KP738571 KP738572 OL191210 OL191219	KP738531 KP738532 OL191459 OL191468	KP738491 KP738492 OL345526 OL345535	OL191307 OL191308 OL191330 OL191339	PP259859 PP259860 PP259910 PP259919	- - - -
Physoschistura brunneana	Myanmar	Shan	Salween	A578	OL191138	OL191386	OL345460	OL191249	PP259906	PP259687
Physoschistura* cf. *rivulicola	Myanmar	Shan	Salween	A6806	OL191223	OL191472	OL345539	OL191343	PP259921	-
Physoschistura* cf. *shuangjiangensis	China	Yunnan	Mekong	A2999	OL191173	OL191423	OL345492	OL191288	-	-

Physoschistura mango	Myanmar	Shan	Salween	A2253	PP279931	PP315764	PP280142	PP280353	PP259805	-
Physoschistura pseudobrunneana	Thailand Thailand	Phayao Chiang Rai	Chao Phraya Mekong	A850 A1356 A1357	OL191155 OL191163 OL191164	OL191403 OL191412 OL191413	OL345474 OL345482 OL345483	OL191266 OL191275 OL191276	PP259964 PP259766 PP259767	- - -
Physoschistura rivulicola	Myanmar	Shan	Salween	A6670	OL191214	OL191463	OL345530	OL191334	PP259915	-
Physoschistura shuangjiangensis	China	Yunnan	Mekong	GenBank	MG238284	MG237990	MG238401	-	-	-
***Physoschistura* sp.**	Myanmar	Shan	Salween	A2256 A7545 A7546	OL191165 KP738600 KP738601	OL191415 KP738560 KP738561	OL345484 KP738520 KP738521	OL191280 OL191355 OL191356	PP259806 PP259943 PP259944	- - -
Pteronemacheilus lucidorsum	Myanmar	Shan	Irrawaddy	A6695 A8465 A8466	OL191215 KP738606 KP738607	OL191464 KP738566 KP738567	OL345531 KP738526 KP738527	OL191335 OL191360 OL191361	PP259916 PP259958 PP259959	- - -
Pteronemacheilus meridionalis	China Laos	Yunnan Louang Namtha	Salween Mekong	A3122 CMK 26015 CMK 25928	PP279958 PP279873 PP279870	PP315795 PP315676 PP315675	- - -	PP280385 PP280250 PP280248	- - -	- - -
***Pteronemacheilus* sp.**	Myanmar	Shan	Irrawaddy	A5851 A5852	OL191208 OL191209	OL191457 OL191458	OL345524 OL345525	OL191328 OL191329	PP259907 PP259908	- -
Sasanidus kermanshahensis	Iran	Kermanshah	Tigris	A5261	PP279994	-	-	PP280435	-	-
Schistura albirostris	China	Yunnan	Irrawaddy	GenBank	MG238242	-	MG238356	-	-	-
Schistura ataranensis	Myanmar Thailand	Ornamental Kanchanaburi	fish trade Ataran	A2560 A5062 A11005	MK886975 MK886998 MK887031	PP315774 PP315829 PP315716	MK886884 MK886907 MK886939	PP280364 PP280429 PP280294	PP259820 PP259879 PP259750	- - -

Schistura aurantiaca	Myanmar Thailand Thailand	Mon Tak Tak	Ataran Mae Klong Salween	A954 A9580 A9584 A11010	MK886950 MK887018 MK887019 MK887032	PP315893 OL191503 PP315894 PP315717	MK886861 MK886926 MK886927 MK886940	PP280523 OL191385 PP280524 PP280295	PP259986 PP259987 PP259988 PP259751	- PP259710 - -
Schistura balteata	Myanmar	Ornamental fish trade		A2554 A2555	MK886971 MK886972	OL191502 PP315773	MK886880 MK886881	OL191384 PP280363	PP259819 -	- -
Schistura beavani	India	No detail	Ganges	GenBank	GQ478448	-	-	-	-	-
Schistura callidora	Myanmar	Shan state	Irrawaddy	A3909 A3910	OL191189 OL191190	OL191438 OL191439	OL345507 OL345508	OL191303 OL191304	- -	- -
Schistura* cf. *nilgiriensis	India	Karnataka	Netravanthi	A9199	PP280057	-	-	-	-	-
Schistura* cf. *scaturigina	India	West Bengal	Rydak I River	A3925 A3926	OL191191 OL191192	OL191440 OL191441	OL345509 OL345510	OL191305 OL191306	PP259856 -	- -
Schistura* cf. *sijuensis	India	Ornamental fish trade		A3698 A3699 A11327	OL191184 OL191185 OL191248	OL191434 OL191435 OL191499	OL345503 OL345504 OL345566	OL191299 OL191300 OL191381	- - -	- - -
Schistura* cf. *vinciguerrae	Myanmar Myanmar	Rakhine Magway	Irrawaddy Irrawaddy	A5557 A6564 A6736	OL191205 OL191211 OL191216	OL191454 OL191460 OL191465	OL345521 OL345527 OL345532	OL191325 OL191331 OL191336	PP259904 PP259911 PP259918	- - -
Schistura cincticauda	Thailand	Tak	Salween	A8312 A8313	MK887016 MK887017	- -	MK886924 MK886925	PP280497 PP280498	PP259953 PP259954	- -
Schistura conirostris	China	Yunnan	Mekong	GenBank	MG238247	MG237953	MG238362	-	MG238061	-
Schistura corica	India	Ornamental fish trade		A6945 A6948 A6953	KP738592 KP738593 KP738594	KP738552 KP738553 KP738554	KP738512 KP738513 KP738514	PP280472 PP280473 PP280475	PP259930 PP259931 PP259932	PP259694 - -
Schistura crabro	Laos	Bolikhamsai	Mekong	CMK 24559	OL191231	OL191480	OL345547	OL191362	PP259982	-
Schistura crocotula	Thailand	Prachuap Khiri Khan	Bang Saphan	A9591 A10513	MK887021 MK887024	PP315895 PP315713	MK886928 MK886931	PP280525 PP280290	PP259989 PP259746	- -

Schistura denisoni	India	Tamil Nadu	Vaigai	A5531 A5532	PP280015 PP280016	- -	- -	- -	- -	- -
Schistura devdedi	Nepal India	No detail Ornamental	Ganges fish trade	A3445 A7541 A7542	PP279972 KP738608 KP738609	PP315808 KP738568 KP738569	PP280175 KP738528 KP738529	PP280403 PP280483 PP280484	- PP259941 PP259942	- - -
Schistura disparizona	China	Yunnan	Salween	GenBank	MG238252	MG238368	MG237958	-	MG238065	-
Schistura hartli	Thailand	Surat Thani	Tapi	A3690	MK886978	PP315809	MK886887	PP280404	PP259855	-
Schistura hoai	Laos	Houaphan	Mekong	CMK25918_1 CMK25918_2	OL191238 OL191239	OL191487 OL191488	OL345554 OL345555	OL191369 OL191370	- -	- -
Schistura hypsiura	Myanmar	Ornamental fish trade		A6922 A6925	KP738584 KP738585	KP738544 KP738545	KP738504 KP738505	PP280467 PP280468	PP259924 PP259925	- -
Schistura indawgyiana	Myanmar	Kachin	Irrawaddy	CMK 25633	PP279865	-	-	-	-	-
Schistura jarutanini	Thailand	Kanchanaburi	Mae Klong	GenBank	NC_031584	-	-	-	-	-
Schistura kloetzliae	Laos	Louang Namtha	Mekong	CMK25994_1 CMK25994_2 GenBank	OL191240 OL191241 MG238237	OL191489 OL191490 MG237945	OL345556 OL345557 MG238351	OL191371 OL191372 -	PP259741 PP259742 -	- - -
Schistura kuehnei	Thailand	Surat Thani	Tapi	A4672 A11261	MK886991 MK887040	PP315825 PP315724	MK886900 PP280099	PP280422 PP280302	PP259871 PP259756	
Schistura longa	China	Yunnan	Salween	GenBank	MG238272	MG237979	MG238389	-	MG238086	-
Schistura mahnerti	Thailand	Mae Hong Son	Salween	A778 A779	PP280030 PP280031	PP315863 PP315864	PP280215 PP280216	PP280486 PP280487	PP259948 PP259949	- -

Schistura malaisei	Myanmar	Kachin	Irrawaddy	CMK25506_1 CMK25506_2	PP279860 PP279861	- PP315696	- -	- -	- -	- -
Schistura mukambbikaensis	India	Karnataka	Netravathi	A9198	PP280056	-	-	-	-	-
Schistura myaekanbawensis	Myanmar	Tanintharyi	Tenasserim	CMK24993	MK887022	PP315695	MK886929	PP280273	PP259731	-
Schistura nilgiriensis	India	Ornamental fish trade		A2626	PP279942	PP315779	PP280152	PP280369	PP259824	-
Schistura notostigma	Sri Lanka	Ornamental fish trade		A7519 A7520 A7521	KP738595 KP738596 KP738597	KP738555 KP738556 KP738557	KP738515 KP738516 KP738517	PP280479 PP280480 PP280481	PP259936 PP259937 PP259938	- - -
Schistura nubigena	Myanmar	Kachin	Irrawaddy	CMK 25509	PP279862	-	-	PP280274	PP259990	-
Schistura obliquofascia	India	No details	No details	GenBank	HM636831	-	-	-	-	-
Schistura paucicincta	Thailand	Tak	Salween	A4946 A4947	OL191203 OL191204	OL191452 OL191453	OL345519 OL345520	OL191321 OL191322	PP259874 PP259875	- -
Schistura poculi	China Thailand	Yunnan Tak	Salween Mae Klong	A2914 A4202 A4203	OL191172 OL191193 OL191194	OL191422 OL191442 OL191443	OL345491 OL345511 OL345512	OL191287 OL191309 OL191310	PP259829 - -	- PP259675 -
Schistura polytaenia	China	Yunnan	Irrawaddy	GenBank	MG238280	MG237986	MG238397	-	MG238092	-
Schistura pridii	Thailand	Ornamental fish trade		A7548 A7549	KP738602 KP738603	KP738562 KP738563	KP738522 KP738523	OL191357 OL191358	PP259945 PP259946	- -

Schistura reticulofasciata	India	Assam	Brahmaputra	GenBank	KY379150	-	-	-	-	-
Schistura robertsi	Thailand	Phang Nga	Tam Nang	A2424	MK886959	OL191501	MK886869	OL191383	PP259810	-
Schistura* cf. *rupecula	Nepal	No detail	Ganges	A3443	PP279971	PP315807	-	PP280402	PP259854	-
Schistura semiarmatus	India	Tamil Nadu	Vaigai	A5529 A5530	PP280013 PP280014	- -	- -	- -	- -	- -
Schistura sikmaensis	China	Yunnan	Irrawaddy	GenBank	JF340405	JF340413	-	-	-	-
Schistura* sp. *Myanmar	Myanmar	Ornamental fish trade		A2569 A2570	PP279938 PP279939	PP315775 PP315776	- -	- -	- -	- -
Schistura thavonei	Laos	Louang Namtha	Mekong	CMK 26066 CMK25944_1	OL191243 OL191244	OL191492 OL191493	OL345559 OL345560	OL191374 OL191375	PP259744 PP259739	- -
Schistura tirapensis	India	Ornamental fish trade		A3703 A3704	OL191187 OL191188	OL191436 OL191437	OL345505 OL345506	OL191301 OL191302	- -	- -
Schistura udomritthiruji	Thailand	Ranong	Kapoe	A2546 A2547	OL191168 MK886969	OL191418 PP315772	OL345487 PP280149	OL191283 -	PP259817 PP259818	PP259661 -
Schistura yingjiangensis	China	Yunnan	Irrawaddy	GenBank	MG238294	MG237999	MG238411	-	MG238103	-
Seminemacheilus ispartensis	Turkey	Isparta	Egidir	A4833 A4834	KP738577 KP738578	KP738537 KP738538	KP738497 KP738498	PP280423 PP280424	PP259872 PP259873	- -
Turcinoemacheilus ekmekciae	Turkey	Diyarbakir	Tigris	A2089	PP279925	PP315758	PP280136	PP280347	PP259801	-
Turcinoemacheilus kosswigi	Iran	No detail	Choman	GenBank	KT861416	-	-	-	-	-
***Turcinoemacheilus* sp. 2**	Iran	Khuzestan	Karoon	GenBank	GQ338827	-	-	-	-	-

OUTGROUP							
Catostomidae							
Cycleptus elongatus	GenBank	NC_031634 14392-15532	EU409613	EU409671	-	EU409639	EU409767
Catostomus commersonii	GenBank	JX488781	EU409612	EU409670	FJ918841	EU409638	EU409766
Hypentelium nigricans	GenBank	AF454909	EU711134	JX470004	JX190418	FJ197033	-
Gyrinocheilidae							
Gyrinocheilus aymonieri	GenBank	NC_008672 14393-15533	EU292682	FJ197122	-	FJ197071	EU409791
Gyrinocheilus pennocki	GenBank	NC_031544 14395-15535	FJ650415	FJ650486	-	FJ650474	FJ650461
Botiidae							
Leptobotia pellegrini	GenBank	NC_031602 14385-15525	EU292683	EU409672	-	EU409640	EU409768
Botia dario	GenBank	KU517084	KU517026	MF681756	-	EU409641	-
Yasuhikotakia morleti	GenBank	NC_031600 14377-15517	FJ650412	FJ650483	-	FJ650471	FJ650457
Syncrossus beauforti	GenBank	NC_031546 14387-15527	FJ650411	FJ650482	-	FJ650470	FJ650456
Vaillantellidae							

Vaillantella maassi				GenBank	NC_008680 14378-15518	EU711132	FJ197080	-	FJ197031	FJ650469
Cobitidae											
Pangio oblonga				GenBank	NC_031592 14386-15526	EU711141	FJ197091	-	FJ197041	FJ650459
Canthophrys gongota				GenBank	NC_031576 14380-15516	FJ650414	FJ650485	-	FJ650473	FJ650460
Cobitis takatsuensis				GenBank	NC_015306 14445-15585	EU409616	EU409675	-	EU409643	EU409771
Cobitis lutheri				GenBank	JN858887	EF508614	KM818238	KM818242	KM583634	-
Cobitis taenia	Germany	Lower Saxonia	Wesser	A1860	EF508508	EF056334	MK608315	OL191279	PP259793	PP259653
Cobitis multifasciata				GenBank	NC_027166 14376-15516	EU409615	EU409674	-	EU409642	EU409770
Cobitis tetralineata				GenBank	KF661673	OK661770	-	OK661564	-	-
Ellopostomatidae											
Ellopostoma mystax				GenBank	NC_031642 14377-15517	FJ650417	FJ650489	-	FJ650477	FJ650464
Balitoridae											
Homaloptera parclitella				GenBank	NC_031634 14392-15532	EU409610	EU409668	-	EU409636	EU409764

Gastromyzonidae							
Sewellia lineolata	GenBank	NC_015534 14375-515	EU409609	EU409667	-	EU409635	EU409763
Cyprinidae							
Barbus callipterus	GenBank	KP712230	FJ531247	FJ531365	-	FJ531345	FJ531317

Table S2.
List of primers used in the present study for amplification and/or sequencing

Locus	Primer name	Primer sequence (5’ - 3’)	Reference
Cyt *b*	Glu-L.Ca14337–14359	GAA GAA CCA CCG TTG TTA TTC AA	Šlechtová et al., 2006
	Thr-H.Ca15568–15548	*ACC TCC RAT CTY CGG ATT ACA*	Šlechtová et al., 2006
	CB-L.Ca14975–14994	CAC GAR ACR GGR TCN AAY AA	Šlechtová et al., 2006
	CB-H.Ca15057–15035	*TCT TTR TAT GAG AAR TAN GGG TG*	Šlechtová et al., 2006
IRBP 2	101F	TCM TGG ACA AYT ACT GCT CAC C	Chen et al., 2008
	109F	AAC TAC TGC TCR CCA GAA AAR C	Chen et al., 2008
	1001R	*GGA AAT GCA TAG TTG TCT GCA A*	Chen et al., 2008
	1162R	*TGG TGG WCT TYA GGC ACT TGT*	Chen et al., 2008
RAG 1	RAG-1F	AGC TGT AGT CAG TAY CAC AAR ATG	Grande et al., 2004
	RAG-RV1	*TCC TGR AAG ATY TTG TAG AA*	Šlechtová et al., 2007
MYH 6	myh6-F507	GGA GAA TCA RTC KGT GCT CAT CA	Li et al., 2007
	myh6-R1322	*CTC ACC ACC ATC CAG TTG AAC AT*	Li et al., 2007
RH 1	RH-1F	CAT ACG AAT ATC CCC AGT ACT ACC	Liu et al., 2012
	RH-28F	TAC GTG CCT ATG TCC AAY GC	Chen et al. 2008
	RH-139F	CNT ATG AAT AYC CTC AGT ACT ACC	Chen et al. 2003
	RH-233F	ATA TGC CTG CCT GGC YGC TTA C	Chen et al. 2008
	RH-1R	*GCT TGT TCA TGC AGA TGT AGA TGC*	Liu et al., 2012
	RH-1039R	*TGC TTG TTC ATG CAG ATG TAG A*	Chen et al. 2003
EGR 3	E3-161F	AAT ATC ATG GAC YTG GGN ATG G	Chen et al. 2008
	E3-1136R	*GGY TTC TTG TCC TTC TGT TTS AG*	Chen et al. 2008

Chen, W.-J., Miya, M., Saitoh, K., Mayden, R.L., 2008. Phylogenetic utility of two existing and four novel nuclear gene loci in reconstructing Tree of Life of ray-finned fishes: The order Cypriniformes (Ostariophysi) as a case study. Gene 423, 125–134.

Grande, T., Laten, H., Lopez, J.A., 2004. Phylogenetic relationships of extant esocid species (Teleostei: Salmoniformes) based on morphological and molecular characters. Copeia 743–757.

Li, C., Orti, G., Zhang, G., Lu, G. 2007. A Practical Approach to Phylogenomics: The Phylogeny of Ray-Finned Fish (Actinopterygii) as a Case Study. BMC Evol. Biol. 7, 44.

Liu, S.-Q.; Mayden, R.L.; Zhang, J.-B.; Yu, D.; Tang, Q.-Y.; Deng, X.; Liu, H.-Z. Phylogenetic relationships of the Cobitoidea (Teleostei: Cypriniformes) inferred from mitochondrial and nuclear genes with analyses of gene evolution. *Gene* **2012**, *508*, 60– 72.

Šlechtová, V., Bohlen, J., Freyhof, J., Ráb, P., 2006. Molecular phylogeny of the Southeast Asian freshwater fish family Botiidae (Teleostei: Cobitoidea) and the origin of polyploidy in their evolution. Mol. Phylogenet. Evol. 39, 529–541.

Šlechtová, V., Bohlen, J. Tan, H.-H. 2007. Families of Cobitoidea (Teleostei; Cypriniformes) as revealed from nuclear genetic data and the position of the mysterious genera Barbucca, Psilorhynchus, Serpenticobitis and Vaillantella. Mol. Phylogenet. Evol. 44, 1358-65.

Table S3.
Alignment attributes and best-fit models. Lengths of alignments, numbers of variable (VP) and parsimony informative (PI) positions and models estimated for all partitions. BEAST and MrBayes models were calculated in Partition Finder 2 (PF2, Lanfear et al., 2016) implemented in PhyloSuite v1.2.2 (Zhang et al., 2020) under AICc criterion, with greedy algorithm (Lanfear et al., 2016) and branch lengths linked. For ML trees the models and partitioning schemes were estimated under BIC by ModelFinder (Kalyaanamoorthy et al. 2017) implemented in IQ tree. The values and models were calculated for both (A) full as well as (B) reduced dataset. Table (C) provides an overview of data attributes for the ingroup dataset only.

A: full dataset

locus		EGR3	IRBP 2	MYH6	RAG1	RH	Cytb
length (bp)		876	831	777	950	844	1122
Variable positions (VP)		341	559	331	503	385	680
% VP		38.93	67.27	42.60	52.95	45.62	60.61
Pars. Informative (PI)		268	483	299	453	333	615
% PI		30.59	58.12	38.48	47.68	39.45	54.81
	partition						
MrBayes models (PF2, AICc)	gene	GTR+I+G	SYM+I+G	GTR+I+G	SYM+I+G	GTR+I+G	GTR+I+G
	1st c.p.	GTR+I+G	GTR+I+G	GTR+I+G	GTR+I+G	SYM+I+G	SYM+I+G
	2nd c.p.	GTR+I+G	GTR+I+G	GTR+I+G	GTR+I+G	GTR+I+G	GTR+I+G
	3rd c.p.	GTR+I+G	SYM+I+G	SYM+G	SYM+I+G	GTR+G	GTR+G
IQ-Tree models (ModelFinder, BIC)	gene	TPM2u+F+I+G4	TIM2e+I+G4	TIM2e+I+G4	TIM2e+I+G4	TIM2e+I+G4	TVM+F+I+G4
	1st c.p.	TIM2e+I+G4	TIM3+F+R3	TN+F+R3	TIM2e+R3	TIM2e+R3	TIM2e+I+G4
	2nd c.p.	TIM3e+R2	TVM+F+G4	TIM2+F+R3	TVMe+I+G4	TPM2+F+R3	TVM+F+R4
	3rd c.p.	GTR+F+G4	TIM2e+R3	TIM2e+R4	TVMe+G4	TIM2+F+G4	TIM2+F+ASC+R5
BEAST models (PF2, AICc)	gene	GTR+I+G+X	GTR+I+G+X	GTR+I+G+X	GTR+I+G+X	GTR+I+G+X	GTR+I+G+X
	1st c.p.	N/E	N/E	N/E	N/E	N/E	N/E
	2nd c.p.	N/E	N/E	N/E	N/E	N/E	N/E
	3rd c.p.	N/E	N/E	N/E	N/E	N/E	N/E

Table S3 continuation

B: reduced dataset

locus		EGR3	IRBP 2	MYH6	RAG1	RH	Cytb
alignment bp		876	831	777	950	844	1122
var.pos.		341	546	327	500	376	681
% V		38.93	65.70	42.08	52.63	44.55	60.70
Pars. Inf.		268	436	284	427	312	579
% PI		30.59	52.47	36.55	44.95	36.97	51.60
	partition						
MrBayes models (PF2, AICc)	gene	GTR+I+G	SYM+I+G	GTR+I+G	SYM+I+G	GTR+I+G	GTR+I+G
	1st c.p.	GTR+I+G	GTR+I+G	GTR+I+G	SYM+I+G	SYM+I+G	SYM+I+G
	2nd c.p.	GTR+I+G	GTR+I+G	GTR+I+G	GTR+I+G	GTR+I+G	GTR+I+G
	3rd c.p.	GTR+I	SYM+I+G	SYM+G	SYM+I+G	GTR+G	GTR+G
IQ-Tree models (ModelFinder, BIC)	gene	HKY+F+I+G4	TIM2e+I+G4	TN+F+I+G4	TIM2e+I+G4	TPM2+F+I+G4	GTR+F+I+G4
	1st c.p.	TIM2+F+I+G4	TIM3+F+G4	K2P+I+G4	TIM2e+I+G4	TNe+I+G4	TIM2e+I+G4
	2nd c.p.	TIM2+F+I+G4	TVM+F+G4	TIM2+F+I+G4	TIM2e+I+G4	TVM+F+I+G4	TVM+F+G4
	3rd c.p.	K2P+G4	TIM2e+G4	TIM2e+G4	TVMe+I+G4	TIM2e+G4	TIM2+F+ASC+G4
BEAST models (PF2, AICc)	gene	GTR+I+G+X	GTR+I+G+X	GTR+I+G+X	GTR+I+G+X	GTR+I+G+X	GTR+I+G+X
	1st c.p.	HKY+I+G+X	TRN+I+G+X	TRN+I+G+X	GTR+I+G+X	GTR+I+G+X	GTR+I+G+X
	2nd c.p.	GTR+I+G+X	GTR+G+X	GTR+I+G+X	GTR+I+G+X	GTR+I+G+X	GTR+I+G+X
	3rd c.p.	GTR+G+X	GTR+I+G+X	GTR+G+X	GTR+I+G+X	GTR+G+X	GTR+G+X

Table S3 continuation

C: full dataset only ingroup

Locus	length (bp)	VP	% VP	PI	% PI
EGR3	876	286	32.65	207	23.63
IRBP 2	831	524	63.06	443	53.31
MYH6	777	313	40.28	286	36.81
RAG1	950	463	48.74	425	44.74
RH	844	352	41.71	307	36.37

Cytb	1122	668	59.54	610	54.37

Lanfear, R., Calcott, B., Ho, S. Y., & Guindon, S. (2012). PartitionFinder: combined selection of partitioning schemes and substitution models for phylogenetic analyses. Molecular biology and evolution, 29(6), 1695-1701.

Lanfear, R., Frandsen, P. B., Wright, A. M., Senfeld, T., Calcott, B. (2016) PartitionFinder 2: new methods for selecting partitioned models of evolution for molecular and morphological phylogenetic analyses. Molecular biology and evolution. DOI: dx.doi.org/10.1093/molbev/msw260

Kalyaanamoorthy S, Minh BQ, Wong TKF, von Haeseler A, Jermiin LS. 2017. ModelFinder: fast model selection for accurate phylogenetic estimates. Nat Methods. 14(6):587–589.

Zhang, D.; Gao, F.; Jakovlić , I.; Zou, H.; Zhang, J.; Li, W.X.; Wang, G.T. PhyloSuite: An integrated and scalable desktop platform for streamlined molecular sequence data management and evolutionary phylogenetics studies. Mol. Ecol. Resour. 2020, 20,348–355

Table S4.
Comparison of biogeographic models in RASP. The last column shows the p-values of the Likelihood Ratio Test. Based on AICc weight (AICc wt), the DEC+J model is recommended as the best fit for our dataset, supported by low p-values indicating the significant influence of the J factor on model likelihood.

Model	LnL	numparams	d	e	j	AICc	AICc_wt	LRT p-val
DEC	-369.3	2	0.0029	0.047	0	742.6	2.0e-26	1.2e-27
DEC+J	-309.9	3	1.0e-12	0.017	0.013	625.8	0.45	
DIVALIKE	-367.2	2	0.0031	0.046	0	738.5	1.5e-25	3.3e-26
DIVALIKE+J	-311.2	3	1.0e-12	0.044	0.014	628.4	0.13	
BAYAREALIKE	-337.9	2	0.0044	0.22	0	679.8	8.7e-13	7.8e-14
BAYAREALIKE+J	-310	3	0.0002	0.15	0.012	626	0.42	